AEROSPACE INFORMATION REPORT

AIR1168™/4	REV. C

Issued 1990-07
Reaffirmed 2004-06
Revised 2016-08
Stabilized 2021-02

Superseding AIR1168/4B

SAE Aerospace Applied Thermodynamics Manual
Ice, Rain, Fog, and Frost Protection

RATIONALE

This document has been determined to contain basic and stable technology which is not dynamic in nature.

STABILIZED NOTICE

This document has been declared "Stabilized" by the SAE AC-9C Aircraft Icing Technology Committee and will no longer be subjected to periodic reviews for currency. Users are responsible for verifying references and continued suitability of technical requirements. Newer technology may exist.

TO PLACE A DOCUMENT ORDER: **Tel: 877-606-7323 (inside USA and Canada)**
Tel: +1 724-776-4970 (outside USA)
Fax: 724-776-0790
Email: CustomerService@sae.org
SAE WEB ADDRESS: **http://www.sae.org**

For more information on this standard, visit
https://www.sae.org/standards/content/AIR1168/4C/

PREFACE

This document is one of 14 Aerospace Information Reports (AIR) of the SAE Aerospace Applied Thermodynamics Manual. The manual was originally published in one volume as ARP1168. The manual provides a reference source for thermodynamics, aerodynamics, fluid dynamics, heat transfer, and properties of materials for the aerospace industry. Procedures and equations commonly used for aerospace applications of these technologies are included.

To maintain consistency with the other 13 reports, unit abbreviations were retained from the previous document, although they may not be the currently recommended abbreviation. An exception is that the current SAE guideline of using “lb” to refer pound mass has been followed. When the Thermodynamics Manual was originally written, most calculations were performed based on pound force and not pound mass. Since most of the equations in this document are more familiar using pound mass, pound mass is used. If using one of the other 13 reports, be aware that “lb” likely represents pound force.

The SAE Aerospace Applied Thermodynamics Manual comprises the following AIR documents.

AIR1168/1 Thermodynamics of Incompressible and Compressible Fluid Flow

AIR1168/2 Heat and Mass Transfer and Air-Water Mixtures

AIR1168/3 Aerothermodynamic Systems Engineering and Design

AIR1168/4 Ice, Rain, Fog, and Frost Protection

AIR1168/5 Aerothermodynamic Test Instrumentation and Measurement

AIR1168/6 Aircraft Fuel Weight Penalty Due to Air Conditioning

AIR1168/7 Aerospace Pressurization System Design

AIR1168/8 Aircraft Fuel Weight Penalty Due to Air Conditioning

AIR1168/9 Thermophysical Properties of the Natural Environment, Gases, Liquids, and Solids

AIR1168/10 Thermophysical Characteristics of Working Fluids and Heat Transfer Fluids

AIR1168/11 Spacecraft Boost and Entry Heat Transfer

AIR1168/12 Spacecraft Thermal Balance

AIR1168/13 Spacecraft Equipment Environmental Control

AIR1168/14 Spacecraft Life Support Systems

F. R. Weiner, formerly of Rockwell International and past chairman of the SAE AC-9B Subcommittee, is commended for his dedication and effort in preparing the errata lists that were used in creating the original 14 documents that comprise AIR1168.

TABLE OF CONTENTS

1. INTRODUCTION

The ability of aircraft to fly in adverse weather conditions is a requirement for most military and commercial aircraft. Ice buildups in critical areas can affect flight safety by adding drag and weight and thus adversely affecting stability.

Supercooled water drops may exist in clouds at ambient temperatures far below the freezing point. When the drops are disturbed by an aircraft flying through them, the drops will impinge and may freeze on airfoil surfaces, radomes, engine inlets, windshields, and other areas, resulting in weight and drag penalties or obstruction of vision through transparent surfaces. Some means, therefore, must be provided to prevent large ice buildups in critical areas.

The inner surfaces of most cockpit transparencies are susceptible to condensation in the form of fog or frost during most normal aircraft operation, particularly when descending from high altitude flight, unless fog and frost protection systems are provided. Fog will form on the inside surface of the windshield whenever that surface is below the cockpit air dew point. If the surface temperature is below 32 °F, frost will form.

Removal of rain from the windshields to maintain pilot visibility is accomplished by hot air jet blast or by windshield wipers. A rain repellent fluid is sometimes used in conjunction with either system for increased rain removal efficiency.

1.1 Scope

This section presents the basic equations for computing ice protection requirements for nontransparent and transparent surfaces and for fog and frost protection of windshields. Simplified graphical presentations suitable for preliminary design and a description of various types of ice, fog, frost, and rain protection systems are also presented.

1.2 Nomenclature

A/B = Semi-length/maximum radius ratio of ellipsoid, dimensionless
A_c = Area of cold side, ft^2
A_f = Body frontal area, ft^2
A_F = Windshield projected area (along line of flight), ft^2
A_h = Area of hot side, ft^2
A_{pa} = Airfoil passage cross-sectional area, ft^2/ft of span-surface
A_w = Wetted surface area, ft^2
a = Nozzle depth, feet
B = Airfoil maximum thickness, feet
b = Passage width, feet
C = Airfoil chord length, or characteristic length, feet
C_{min} = Minimum heat capacity between hot and cold side, Btu/h-°F
c_w = Specific heat of water = 1.0 Btu/lb-°F
D_h = Passage hydraulic diameter, feet
d_{med} = Volume-median drop diameter, µm (3.94×10^{-5} inches)
d = Passage depth, feet
e = Base of the Napierian (natural) logarithm, 2.718
exp = Exponent
E_m = Total water catch efficiency, dimensionless
F = Wettedness factor, dimensionless
G_f = Percent freeze point depressant by weight in final mixture, %
G_i = Percent freeze point depressant by weight in initial mixture, %
h_c = Hot side heat transfer coefficient, Btu/h-ft^2-°F
h_i = Internal (or passage) heat transfer coefficient, Btu/h-ft^2-°F
h_o = External heat transfer coefficient, Btu/h-ft^2-°F
h_oS_o = External film conductance, Btu/h-°F-ft of span per surface
k = Thermal conductivity, Btu-in/h-ft^2-°F
k_a = Thermal conductivity of air at nozzle, Btu/h-ft-°F
k_g = Thermal conductivity of glass, 6 Btu-in/h-ft^2-°F
k_p = Thermal conductivity of plastic 1.5 Btu-in/h-ft^2-°F
k_o = Thermal conductivity of air at freestream static temperature, Btu/h-ft-°F
K_o = Modified inertia parameter, dimensionless
K_1 = Pressure correction (see Figure 11), dimensionless

K_a = Average power/power at control point (Equation 48), dimensionless
K_h = Power at hot spot/power at control point (Equation 49), dimensionless
K_m = Average power/power at hot spot (Equation 50), dimensionless
L_e = Latent heat of evaporation, Btu/lb
L_{eq} = Equivalent passage length, feet
L_n = Nozzle length, feet
LWC = Cloud liquid water content, g/m^3
L_x = Length, feet
M = Total water catch, lb/h, or in the case of an airfoil, lb/h-ft of span
M_β = Local water catch, lb/h-ft^2
M_n = Mach number, dimensionless
M_w = Windshield water catch, lb/h-ft^2 of surface area
N_{Nu} = Nusselt number, dimensionless
$N_{(Re,d)}$ = Freestream Reynolds number based upon water drop diameter, dimensionless
$N_{(Re,o)}$ = Freestream Reynolds number based upon body length, dimensionless
$N_{(Re,s)}$ = Local surface Reynolds number based upon surface distance from stagnation point, dimensionless
n = Number of heat transfer passages per foot of span per surface
P_{cb} = Cabin pressure, inch Hg
P_{amb} = Ambient (freestream) static pressure, psia or inch Hg
p_{sk} = Saturation pressure of vapor at t_{sk}, psia
p_w = Saturation pressure of water vapor at t_w, psia
p_{ws} = Saturation pressure of water vapor, inch Hg
Q_i = Heat loss to inside, Btu/h-ft^2
Q_o = Heat loss to outside, Btu/h-ft^2
Q_t = Total heat loss, Btu/h-ft^2
q = Heat flow, Btu/h
q_a = Average heat flow to exterior surface, Btu/h-ft^2
r = Maximum radius of conical body, feet
r = Recovery factor, dimensionless
S = Surface area, ft^2
s_b = Impingement limit on any body, feet, inches
S_L = Airfoil lower surface impingement limit, ratio to chord, dimensionless
S_o = External heat transfer area, ft^2, or in the case of an airfoil, ft^2/ft of span per surface
s_L = Airfoil lower surface impingement limit, feet, inches
S_m = Total area of impingement divided by body frontal area, dimensionless
S_U = Airfoil upper surface impingement ratio, ratio to chord, dimensionless
s = Surface distance from stagnation point, feet, inches
s_U = Airfoil upper surface impingement limit, feet, inches
T_{amb} = Ambient (freestream) static temperature, °R
T_m = Mean temperature between wall and fluid, °R
T_{bl} = Temperature of boundary layer, °R
t_{aw} = Adiabatic wall temperature, °F
t_c = Temperature at control point, °F
t_{cb} = Cabin temperature, °F
t_{ex} = Passage exit air temperature, °F
t_{fa} = Temperature of film average, °F
t_h = Hot spot temperature, °F
t_{in} = Passage inlet air temperature, °F
t_j = Temperature at a point downstream of nozzle, °F
t_n = Nozzle temperature, °F
t_s = Effective outside surface temperature, °F
t_{si} = Inside surface temperature, °F
t_{sk} = Skin temperature, °F
t_w = Total temperature of atmospheric water, °F
thick = Thickness of piccolo tube
U_h = Heat transfer coefficient hot side, Btu/h-ft^2-°F
U_i = Heat transfer coefficient to inside, Btu/h-ft^2-°F
U_o = Heat transfer coefficient to outside, Btu/h-ft^2-°F
U_{ov} = Overall heat transfer coefficient, Btu/h-ft^2-°F

V = Freestream velocity, ft/s
v = Freestream velocity, knots TAS
V_j = Velocity at distance x, ft/s
V_o = Velocity at nozzle, ft/s
W = Mass flow of air, lb/s
W_f = Liquid flow rate, lb/h-ft^2 surface area
W_s = Moisture content, lb/lb dry air
w_{pa} = Passage air flow, lb/h-ft of span per surface
ΔX = Total windshield thickness, inches
x = Distance from nozzle, feet
Δx_i = Distance from film to inner surface, inches
Δx_o = Distance from film to outer surface, inches
Y = Correction factor for passage fin effect, dimensionless
Z = Correction factor for passage aspect ratio, dimensionless
α = Angle of attack, deg
β = Local catch efficiency, dimensionless
β_{max} = Local catch efficiency at stagnation line, dimensionless
Φ_o = Cone semivertex angle, deg
Γ = Local catch parameter on cones, dimensionless
μ_o = Absolute viscosity of air at freestream static temperature or nozzle temperature, lb/s-ft
Ψ = Scale modulus, dimensionless
η_t = Decay ratio, dimensionless
ρ_o = Ambient air density, lb/ft^3
ρw = Water drop air density, lb/ft3

1.3 Common Abbreviations

AAFTR	Army Air Forces Technical Report
AC	Alternating current
Aer	Bureau of Aeronautics, Department of the Navy
AF	Air Force
ASG	Aeronautical Systems Group
Btu	British thermal units
cc	Cubic centimeters
DC	Direct current
CFR	Code of Federal Regulations
deg	Degree(s)
exp	Exponent
°F	Degrees Fahrenheit
FAA	Federal Aviation Administration
ft	Feet
g	Gram(s)
Hg	Mercury
h	Hour(s)
in	Inch(es)
IVR	Inlet velocity ratio
lb	Pound(s) mass
lb_f	Pound(s) force
LE	Leading edge
LWC	Liquid water content
m	Meter(s)
max	Maximum (in tables)
min	Minute(s)
mph	Miles per hour
nmi	Nautical mile, international
NACA	National Advisory Committee for Aeronautics

%	Percent
p. (pp.)	Page(s)
Proc.	Proceedings
PS	Parting strip
psi	Pounds force per square inch
psia	Pounds force per square inch absolute
PT	Point
°R	Degrees Rankine
RM	Research Memorandum
s	Second(s)
SI	International System of Units
STAG.	Stagnation
TAS	True Air Speed
TEMP.	Temperature
TN	Technical Note
TR	Technical Report
Typ.	Typical
U.S.	United States
USAF	United States Air Force
W	Watt(s)
WADC	Wright Air Development Center
µm	Micrometer, 10^{-6} meter (formerly known as micron)

1.4 Definition of Terms

The following terms are used in this discussion:

1. Icing Cloud: A cloud containing supercooled water drops of sufficient concentration and size to produce ice on an airborne aircraft's surface.

2. Liquid Water Content: Liquid water content is the total mass of water contained in liquid drops within a unit volume or mass of cloud or precipitation, usually given in units of grams of water per cubic meter or kilogram of dry air (g/m^3, g/kg) of air.

3. Median Volumetric Diameter (MVD): The drop diameter which divides the total liquid water content present in the drop distribution in half, i.e., half the water volume will be in larger drops and half the volume in smaller drops.

4. Maximum Drop Size: Maximum drop size is the size of a drop which is larger than 95% of the drops. It is approximately double the volume median drop size and is used to determine impingement limits.

5. Local Water Catch: Local water catch is the point-by-point distribution of water (or ice), in lb/h-ft^2 surface area, over the impingement area.

6. Total Water Catch: Total water catch is the total amount of water (or ice), in lb/h, that impinges on the aircraft surface. It is the integrated value of the local catch. For a two-dimensional body (for example, on a wing) the total catch is more conveniently expressed in terms of a unit span.

7. Total Catch Efficiency: Total catch efficiency is the total water catch on a body divided by the amount of water contained in the volume of air swept out by the frontal area of the body.

8. Local Catch Efficiency: Local catch efficiency is the local catch divided by that which would be caught on 1 ft^2 of surface area with a catch efficiency of unity.

9. Impingement Limit: The impingement limit is the farthest aft location on a body at which water drops impact. This applies to both the upper or lower surface for a body such as an airfoil. This distance can be measured either as the x distance from the leading edge or as the surface distance from the stagnation point.

10. Anti-ice: The prevention of ice accumulation on a protected surface.

11. Deice: The periodic shedding of ice accretions by destroying the bond between the ice and the protected surface.

2. ICE PROTECTION OF NONTRANSPARENT SURFACES

Various methods have been developed for aircraft ice protection of nontransparent surfaces. The earliest practical method was to use inflatable rubber pneumatic boots which, when inflated, broke the bond between the ice and the surface, thus allowing aerodynamic forces to blow the ice away. This method, because of its simplicity, is still employed on many aircraft.

Recent developments include electromechanical methods that break the bond of the ice to the surface. Since the pulse used is instantaneous and the power can be stored, this device requires a relatively small amount of total power to operate.

Another form of ice protection uses glycol or alcohol pumped in a thin film over the protected surface, thus lowering the freezing point and preventing the formation of ice.

An effective method of ice protection is to use thermal energy, either hot air or electrical. Many all-weather aircraft employ thermal ice protection systems.

The thermal energy required for ice protection can be obtained in two ways:

1. Hot air, either heated ram air or compressor bleed air, passed through passages integral with the surface being heated.

2. Electrical resistance heating elements embedded just below the surface being heated.

In either case, thermal ice protection results in aircraft weight and performance penalties related to system capability, and makes necessary the accurate prediction of ice protection required for a given application.

The calculation of ice protection requirements can be tedious, in some cases requiring extensive trial and error experiments or computer codes. It is possible, however, to rearrange the water catch and heat and mass transfer equations into forms that permit graphical presentation of the various parameters, thus reducing the number of calculations.

This AIR discusses these graphical presentations and includes illustrative problems of typical ice protection systems to enable the designer to make calculations of system requirements. The methods presented here, though approximate, have produced good correlation in both icing tunnel tests and natural icing flights. Even though more sophisticated computer programs are available, these methods are still in use and widely accepted. Reference 18 is dedicated to computer codes and lists many of the simulation codes and discusses their capabilities.

Analysis of thermal ice protection systems can be undertaken with those familiar with thermodynamics using the techniques provided in this AIR. Other types of ice protection systems require specialized tools developed by those supplying those systems. A more detailed description of other types of ice protection systems including those mentioned here can be found in Reference 33. This AIR will provide techniques and methods of analysis related only to thermal ice protection systems. As indicated other systems require specialized analysis tools that are often proprietary to the companies providing those systems.

3. METHODS OF THERMAL ICE PROTECTION

3.1 Fully Evaporative Anti-Icing

Fully evaporative anti-icing systems, either electrical or hot air, are used for wing and empennage surfaces and, in the case of turbine powered aircraft, for engine air intake systems. For electrical systems, electrical-resistance heating elements are installed on the aircraft in areas requiring ice protection. For hot air systems, heated air is directed at or along the inner surfaces of such areas. Energy requirements are determined by assuming full evaporation of all impinging water under the severest condition which the aircraft is expected to encounter (see Section 8).

In piston engine powered aircraft, ram air can be heated either by a combustion heater or by being passed through an engine exhaust air heat exchanger. However, ram air systems are limited in their evaporative capabilities, especially in light of the latest civil and military specifications. In turbine engine powered aircraft, compressor bleed air is usually utilized to provide adequate ice protection. Compressor bleed air systems are lighter than equivalent heated ram air systems, since they can use the same bleed manifolds required for engine starting.

3.2 Running Wet Anti-Icing

Heat requirements, either electrical or hot air for running wet anti-icing, are based upon the maintenance of a surface temperature just above freezing, thus allowing some of the impinging water to run back and freeze aft of the heated area. This technique is employed for surfaces where the effects of ice buildups aft of the heated area can be tolerated (e.g., radomes and spinners). It is also used in (1) turbine engine inlet ducts where the runback is permitted to enter the engine, and (2) on the duct lips of all-weather supersonic aircraft where only limited protection is required.

3.3 Cyclic Deicing

Cyclic deicing is the periodic shedding of small ice buildups. In thermal deicing, the ice-airfoil interface is melted by a high rate of heat input; the adhesion at the ice-airfoil interface becomes zero and aerodynamic or centrifugal forces remove the ice. With the advent of lightweight AC systems for aircraft application, electrical resistance heating elements are also used for deicing. Electrothermal systems are used primarily for airfoil surfaces (since small ice buildups here may not be detrimental to airplane performance or handling qualities) or on propeller and helicopter blades where other means are impractical. Electrothermal deicing requires the least amount of heat of all thermal ice protection systems, but this advantage is partially offset by the aerodynamic penalties incurred during the "heat-off" period.

4. EXTERNAL FACTORS AFFECTING HEAT REQUIREMENTS

4.1 Water Catch and Impingement Limits

4.1.1 Methods of Determination

Water catch parameters on a body may be determined either experimentally in an icing wind tunnel or analytically. The experimental technique (Reference 1) is to allow a short burst of dye spray of known quantity and drop distribution to impinge on blotting paper that has been taped to the body for this purpose. A colorimetric analysis of the paper is performed to determine the local and total catch efficiencies and impingement limits, the latter requiring correction for model scale effects. Alternately, the collection efficiency may be determined experimentally following icing exposure during rime conditions for a short period. The exposure time is just sufficient to measure reliably variations in ice thickness within the impingement area, and not long enough for secondary effects such as ice feather growth near the impingement limits. The local collection efficiency can be computed knowing the local ice thickness, the airspeed, the exposure time, and the freestream LWC.

The analytical approach (Reference 2) is the direct solution of the appropriate differential equations. This method has produced good correlation with icing tunnel results, both for water catch and impingement limits, when the flow field could be calculated accurately. Because of the high cost of tunnel programs, the bulk of available water catch data for simple body shapes has been obtained analytically.

4.1.2 Airfoils

4.1.2.1 Total Water Catch

The fundamental equation for total water catch is

$$M = 0.38vB(LWC)E_m \qquad \text{(Eq. 1)}$$

For a given volume median drop size, ambient temperature, and altitude, water catch efficiency, E_m, is a function of velocity, airfoil shape, and thickness. References 2 and 3 present curves for the determination of E_m for several 15% thick airfoils, obtained from a differential analyzer, based on two parameters, a drop Reynolds number $N_{(Re,d)}$, and a scale modulus Ψ. Large amounts of information have been accumulated for numerous classical shapes such as rectangles, ribbons, spheres, cylinders, and ellipsoids, as well as for airfoils.

A simplified parameter called a "Modified Inertia Parameter, K_o," was developed in References 4 and 5. The use of this K_o parameter permits correlation into a set of universal K_o plots of most of the published drop trajectory data of (1) water catch efficiency (E_m), and upper and lower limits of ice impingement (S_U, S_L) for airfoils, rectangles, ribbons, spheres, cylinders, radomes, ellipsoids, elbows, cones, and engine inlets; and (2) local stagnation line impingement efficiency (β_{max}) for ellipsoids, spheres, cylinders, and rectangular half-bodies. Use of the K_o correlation is considered justified by the small loss in accuracy versus the large condensation in data presentation made possible by its use, however, the calculation of K_0 is also feasible (see Equation 2).

Efficiency of water catch (E_m) data for airfoils, engine inlets, and many geometrical shapes is shown in Figure 1 (taken from References 6 and 7) as a function of the modified inertia parameter K_o. Each geometric shape is represented by a single curve. It should be noted that the efficiency of water catch can be greater than 1.0 (that is, >100%) because E_m is strictly defined as the dimensionless ratio of the amount of water intercepted by a body to the amount of water contained in the volume of cloud swept by the body when at α = 0 degrees.

At angles of attack greater than 0 degrees, the amount of water intercepted by an airfoil may be larger than the amount of water contained in the volume of cloud swept out by the airfoil when at α = 0 degrees. The plots shown in Figure 1 are generally within ±10% of the original data for the practical range of drop Reynolds numbers from 100 to 250.

The collection efficiency may be larger than 100%. As an example, drops that miss an aircraft radome and travel close to the fuselage and produce a local high concentration downstream may impact a portion of an air data probe that protrudes a short distance from the surface. These effects can be predicted with reasonable reliability by advanced computational tools that take into account the full three-dimensional flow and drop trajectory effects.

The K_o factor may be evaluated either using Figure 2 or by the following equation:

$$K_o = \left(\left[\frac{d_{med}^2 v \rho_w}{C \mu_o}\right]\right)\left[N_{(Re,d)}^{-2/3} - \frac{\sqrt{6}}{N_{(Re,d)}} \arctan\left(\frac{N_{(Re,d)}^{1/3}}{\sqrt{6}}\right)\right] \quad \text{(Eq. 2)}$$

Figure 3 presents a plot of M/LWC for a 15% Joukowski airfoil as a function of true air speed and airfoil thickness, for α = 4 degrees and 20 µm water drops. Plots of this type are accurate for only one angle of attack, drop diameter, altitude, and airfoil thickness ratio, but may be used as a range of altitudes and airfoil thickness ratios in making preliminary design first approximations for subsonic airfoils. The more refined K_o and E_m method is preferred for greater accuracy. A comprehensive summary, including experimental data, can be found in Reference 8. Alternately, recent computational tools have simplified the steps for these predictions, but they require familiarity and experience.

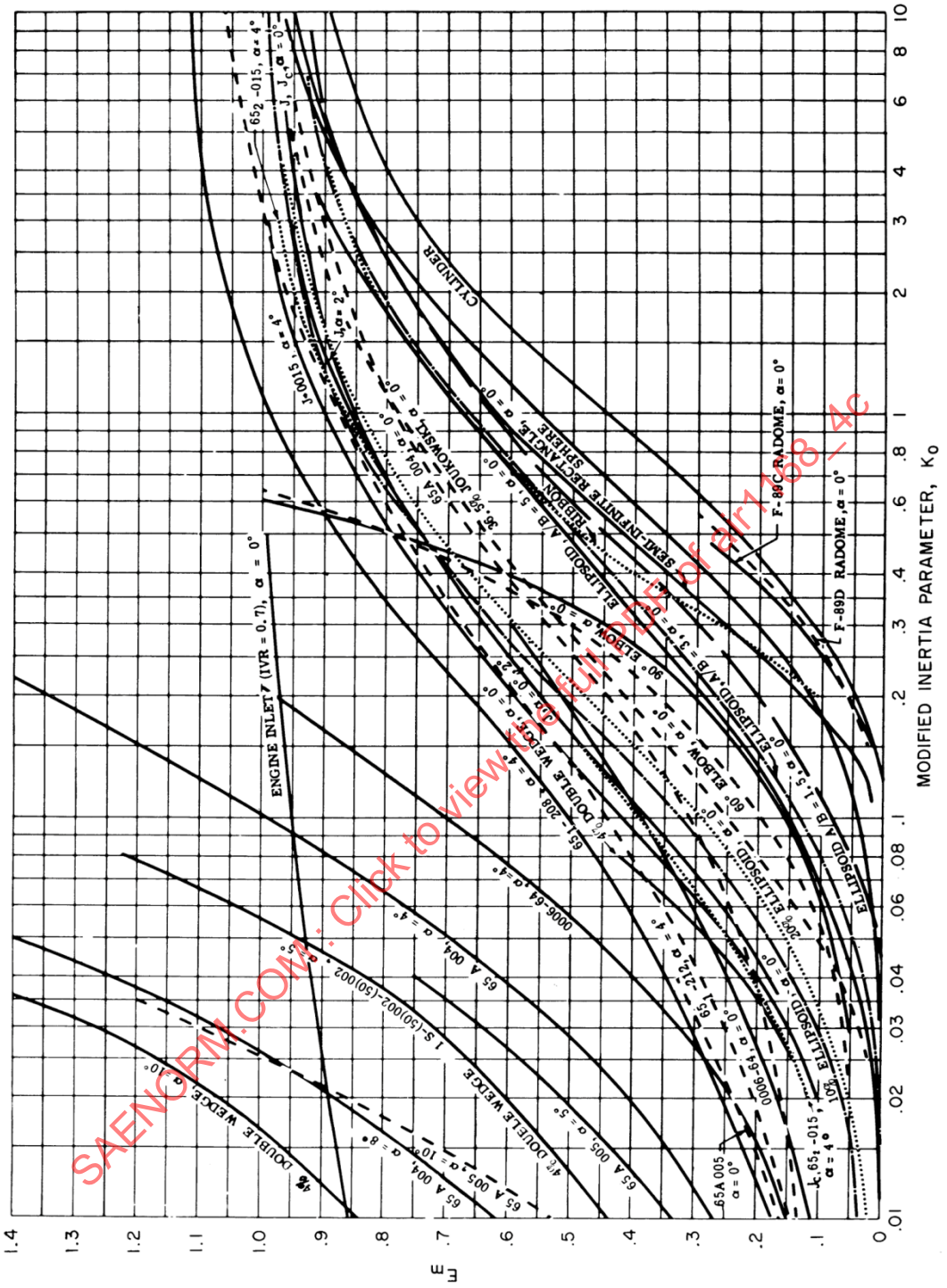

Figure 1 - Water catch efficiencies for various airfoils and geometric shapes
(J refers to Joukowski 0015 airfoil, subscript c means cambered; References 6 and 7)

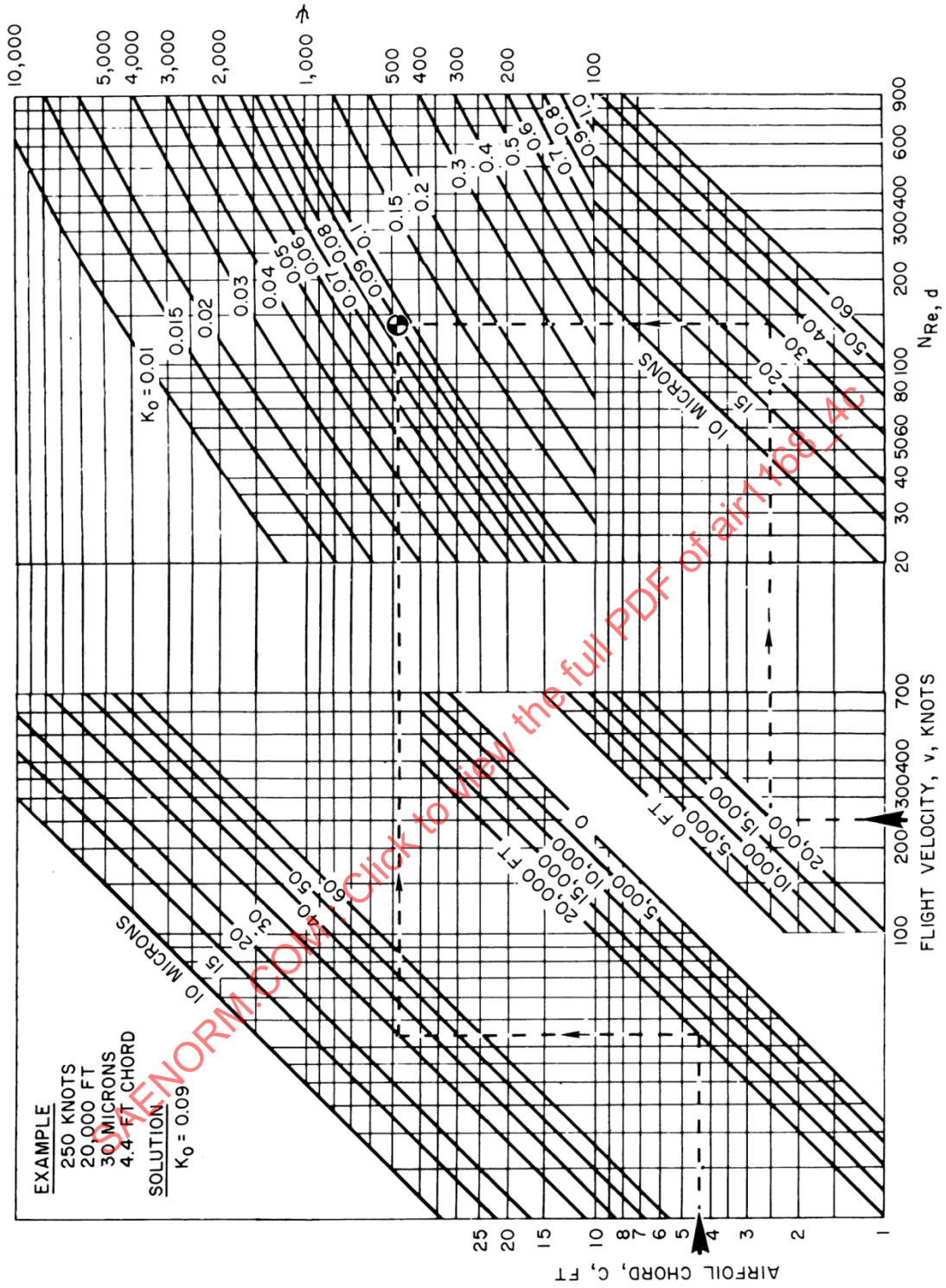

Figure 2 - Graphical solution of K_o for 15 °F ambient air temperature (References 6 and 7)

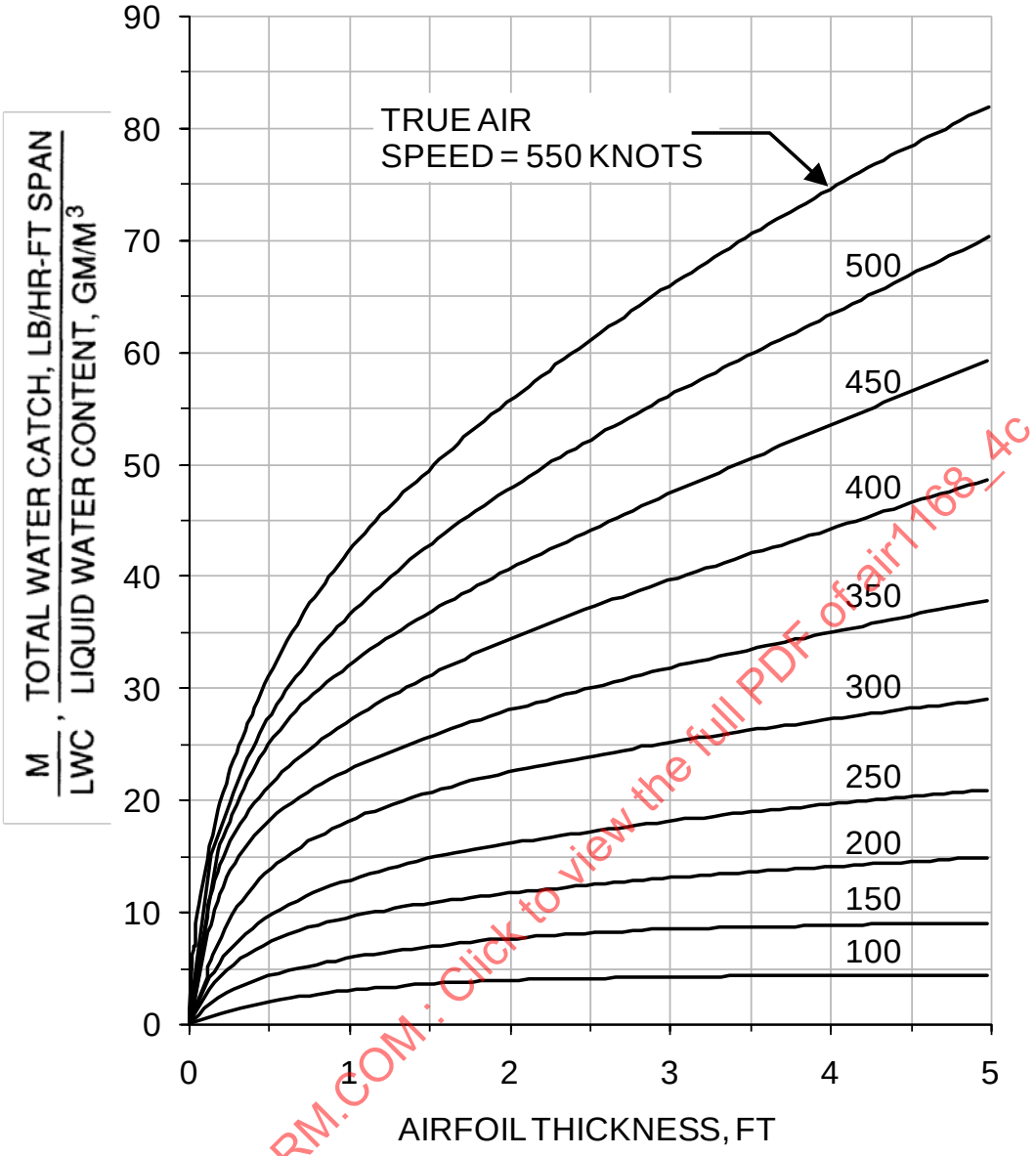

Figure 3 - Airfoil total catch typical for 6 to 16% thick airfoils at α = 4 degrees 20 µm volume median drops (all altitudes: strictly true for 10000 feet and approximately, within 10%, true between sea level and 20000 feet)

4.1.2.2 Local Water Catch Distribution and Impingement Limits

The formula for local water catch, analogous to Equation 1, is:

$$M_{\beta} = 0.38v(LWC)\beta \qquad \text{(Eq. 3)}$$

Local water catch efficiency, β, is a complex function of drop size, airfoil geometry, and freestream conditions. Consequently, it is not possible to construct a set of semi-universal curves using the method from Reference 9, as it is for total water catch. Reference 8 presents curves for determining local water catch efficiencies for several airfoil sections at various angles of attack. Figure 4 shows the maximum water catch efficiency at the stagnation line, β_{max}, versus the modified inertial parameter, K_o, for three ellipsoids and a sphere, cylinder, and rectangular halfbody (from References 6 and 7).

Airfoil impingement limits, too, are a complex function of maximum drop size, airfoil geometry, and freestream conditions. These limits are used to determine how far aft of the leading edge the surface requires protection. References 2 and 3 and 6 through 8 present curves for obtaining impingement limits for several airfoil sections at various angles of attack. Aviation regulatory agencies specify a drop size as a mean volumetric diameter within a distribution of drop sizes. In the determination of impingement limits, a single drop size or a distribution has been used. The procedure is simple using existing computational tools. It should be noted that large drops that exist near the edge of a distribution impinge farther aft on the surface compared to the nominal drop size. However, they contribute a small percentage of total cloud water content. The specific application dictates whether a single drop size or a distribution should be used in analyzing impingement limits.

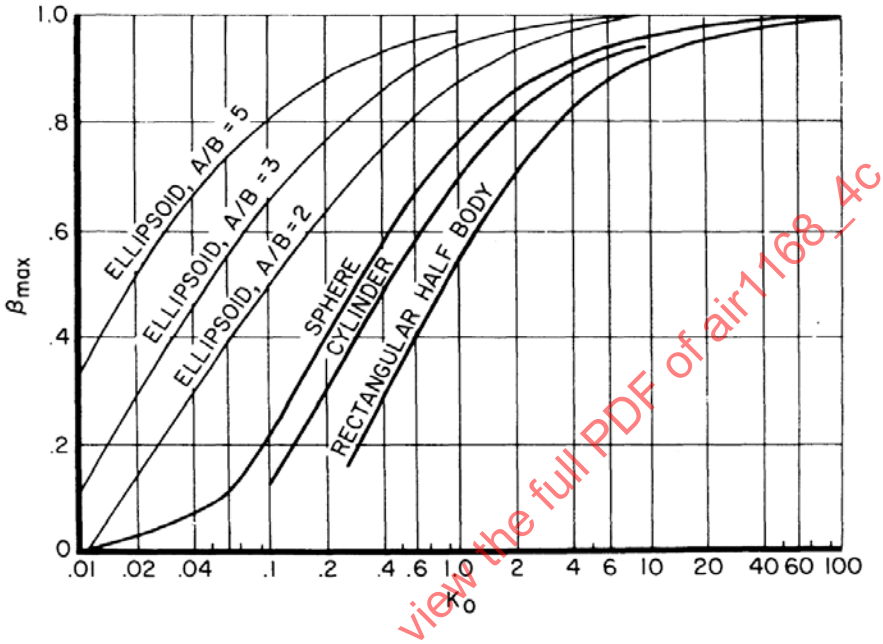

Figure 4 - Maximum water catch efficiencies at the stagnation line, α = 0 degrees

As an example, Figure 5 shows the impingement limits for an NACA 65_2-015 airfoil at α = 4 degrees, and for a symmetrical 15% airfoil at α = 0 degrees. Over the range of airfoil geometries of interest, impingement limits appear to be only moderately sensitive to changes in percent thickness and camber, but are very sensitive to changes in angle of attack, this latter effect being roughly parabolic.

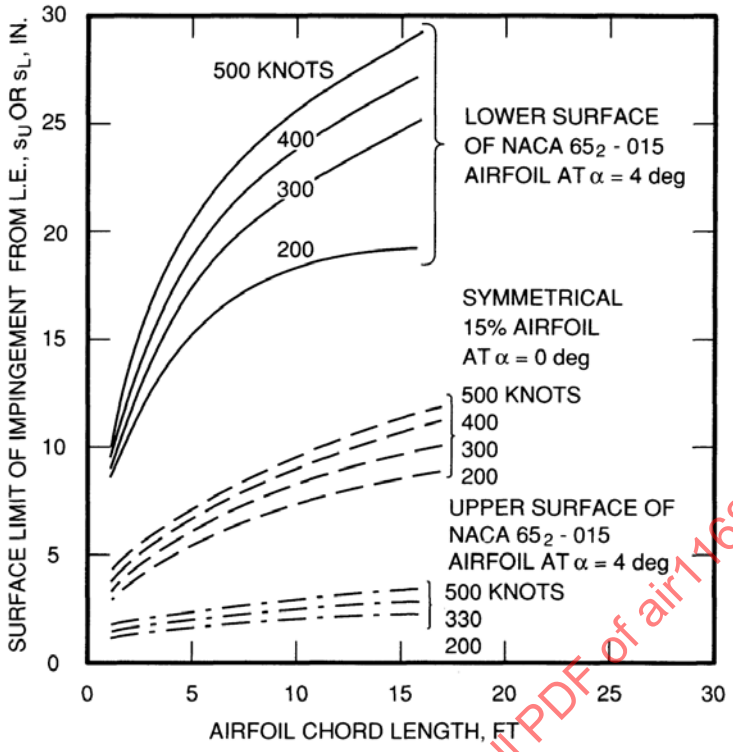

Figure 5 - Airfoil impingement limits for 40 µm maximum (20 µm volume median) drops (all altitudes: strictly true for a particular altitude and approximately, within 10%, true between sea level and 20000 feet)

Figures 6 and 7 show the upper and lower limits of ice impingement (S_U, S_L), as simplified by the K_o correlation (taken from References 6 and 7). The tendency of thin airfoils, at large angles of attack ($\alpha \geq 4$ degrees), to accumulate ice up to the mid-chord on the lower surface under conditions of large K_o (large drop size, high speed, small chord length) is clearly apparent.

The method of presentation in Figures 1, 6, and 7 permits interpolation or extrapolation to other airfoil thicknesses and angles of attack for which water drop trajectory data are not known.

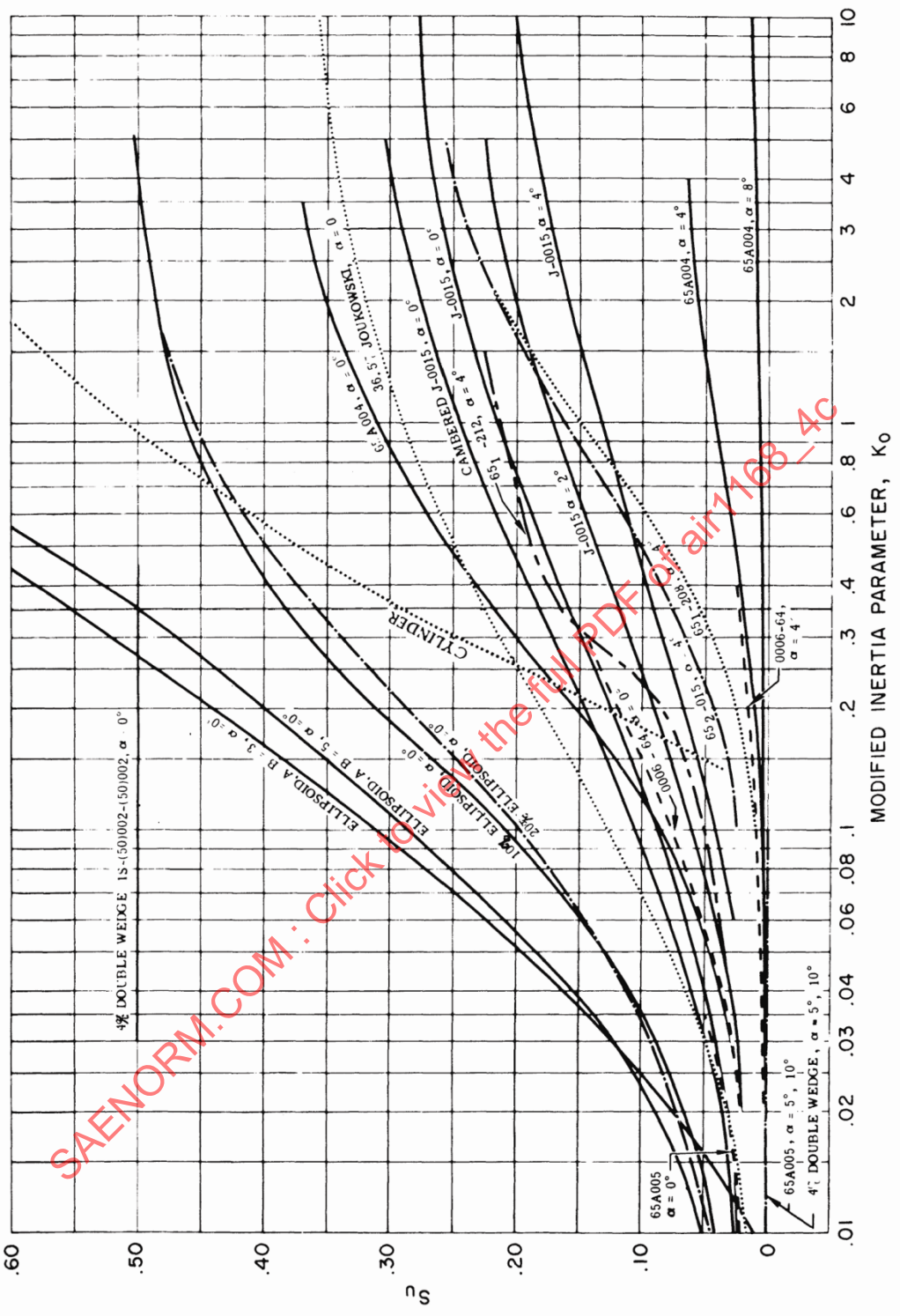

Figure 6 - Water drop tangent trajectories on upper surface
Note: S_u > 0.80 for cones (α = 0 degrees, any vertex angle) for K_o > 0.04

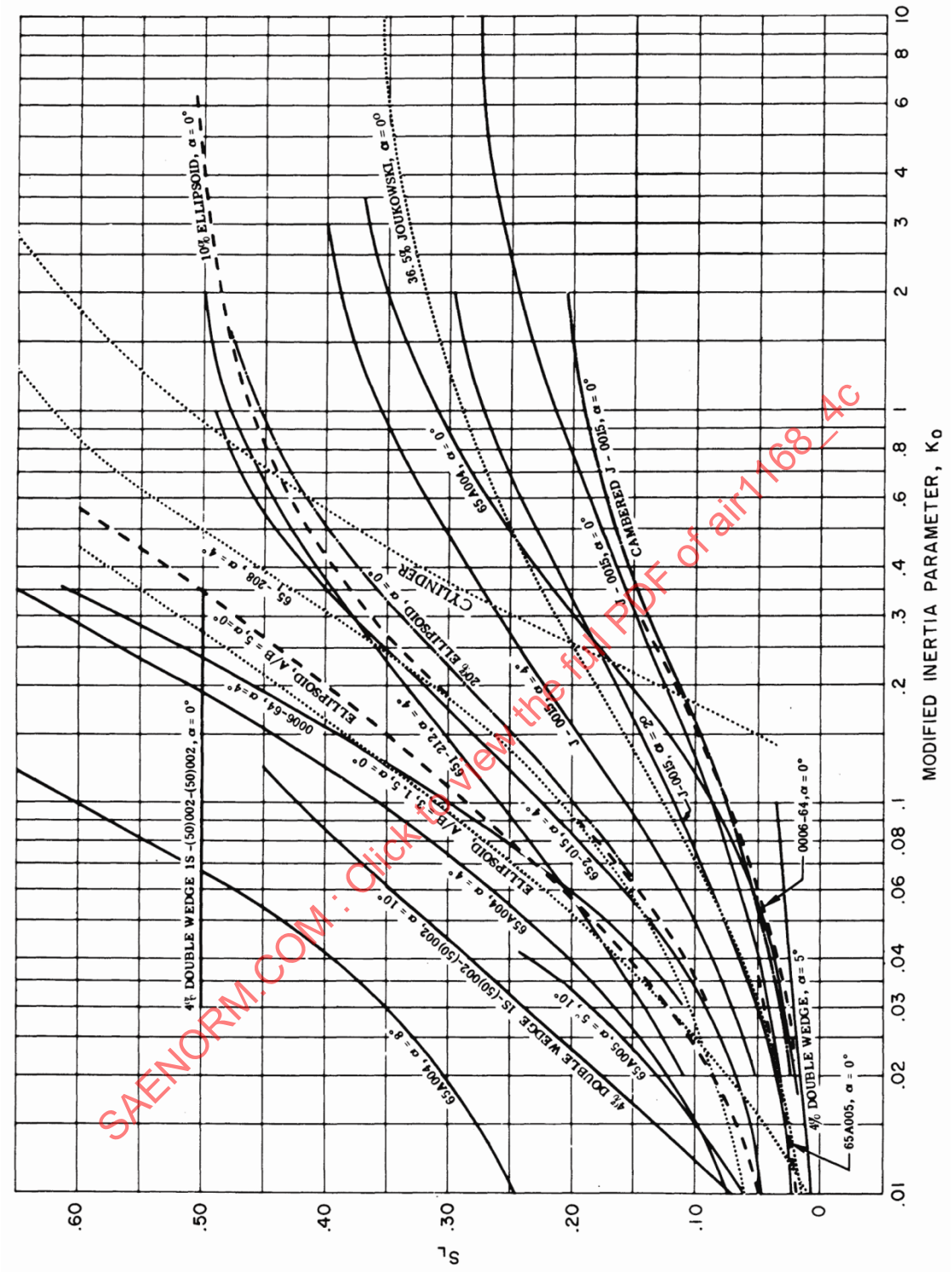

Figure 7 - Water drop tangent trajectories on lower surface
Note: SL > 0.80 for cones (α = 0 degrees, any vertex angle) for K_o > 0.04

4.1.3 Bodies of Revolution

The equation analogous to Equation 1 for bodies of revolution is

$$M = 0.38vA_f(LWC)E_m \quad \text{(Eq. 4)}$$

where A_f is the frontal area of the body. Figure 8 shows cone water catch efficiencies as obtained from Reference 9, plotted as a function of velocity and body (radome, spinner, and so forth) length. In the same manner, it is possible to plot $\beta_{max}/\sin\Phi_o$ where Φ_o is the cone semivertex angle (Figure 8) and s_b is the impingement limit (Figure 9).

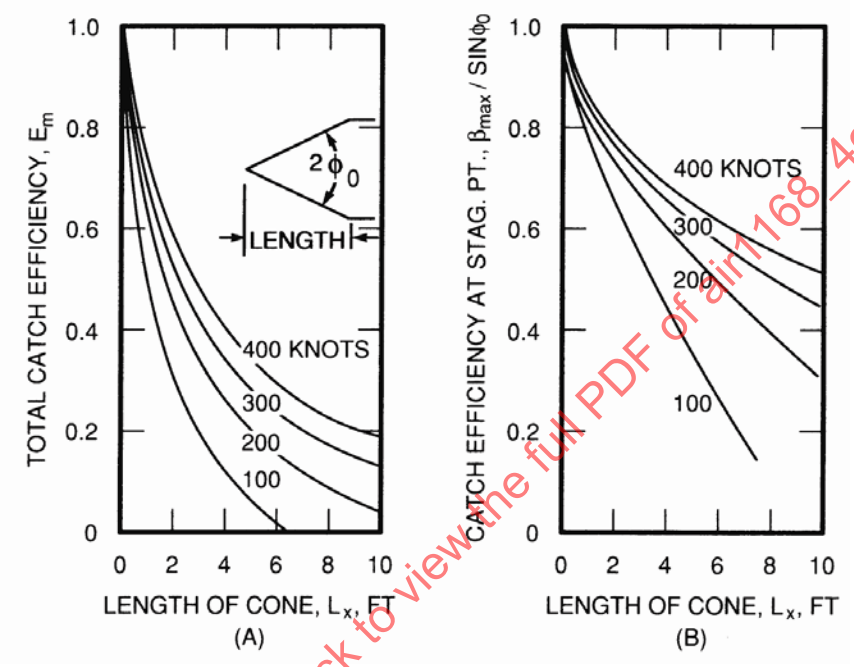

Figure 8 - Catch efficiency on cones for 20 µm volume median drops (A) - Total, (B) - Stagnation point (all altitudes: strictly true for 10000 feet altitude and approximately, within 10%, true between sea level and 20000 feet)

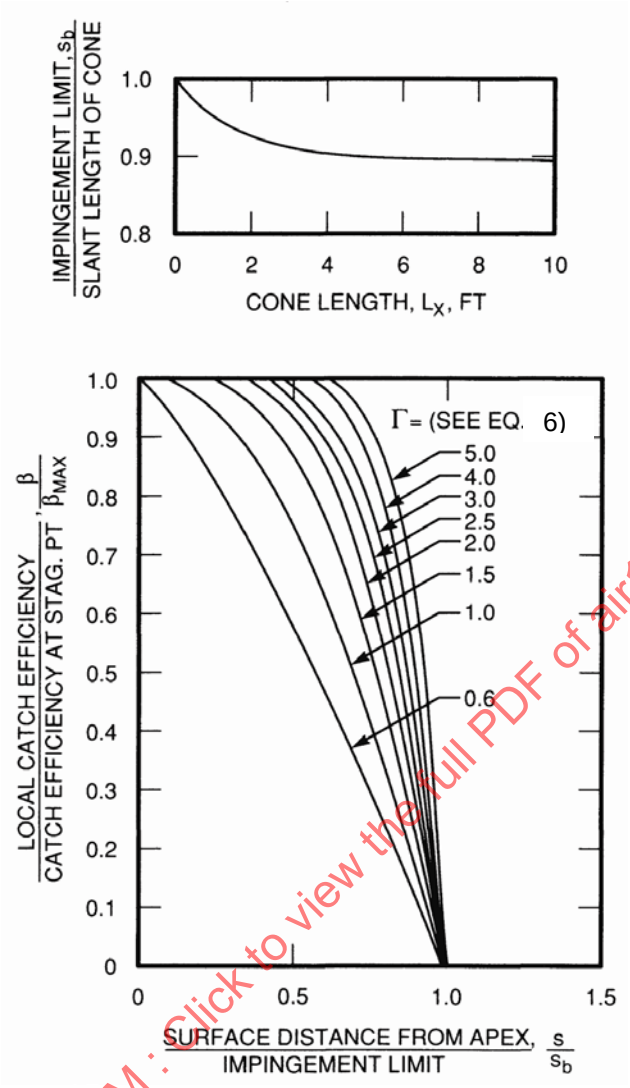

Figure 9 - Local catch distribution (bottom) and impingement limits (top) on cones for 20 µm volume median drop diameter.
Note: impingement limits are fairly insensitive to changes in altitude and velocity.

The cones analyzed in Reference 9 are rounded at the base, as shown in Figure 10, where s_b = Impingement limit and $r = L_x \sin\Phi_o$.

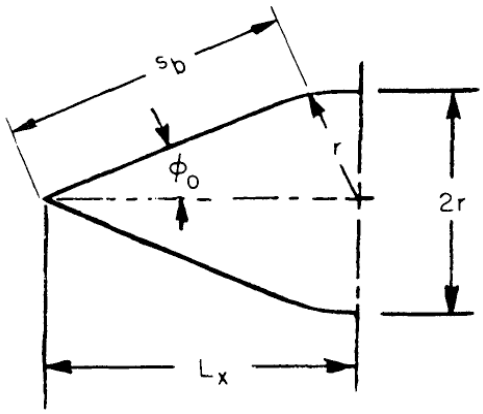

Figure 10 - Cone geometry

Then

$$A_f = \pi L_x^2 \sin^2 \Phi_o \quad \text{(Eq. 5)}$$

To obtain local catch distributions (Figure 9), it is necessary to compute the quantity Γ, where

$$\Gamma = \frac{E_m}{\beta_{max} S_m - E_m} \quad \text{(Eq. 6)}$$

The factor S_m is the impingement area divided by the cone frontal area. Using the cone geometry of the sketch,

$$S_m = \frac{(s_b / L_x)^2}{\sin \Phi_o} \quad \text{(Eq. 7)}$$

Catch rates for ellipsoids may be obtained from the previous figures and also from Reference 9.

4.2 External Heat Transfer Coefficients

4.2.1 Airfoils

4.2.1.1 Local

The calculation of local heat transfer coefficients requires knowledge of the velocity and static pressure distributions over the airfoil. Since this latter subject is covered in Reference 10 as well as in standard aerodynamic textbooks, it will not be presented here.

Laminar heat transfer coefficients are computed by using the Eckert wedge solution, which assumes that laminar heat transfer coefficients on an airfoil are the same as those on a wedge at the same distance from the stagnation point, provided the stream velocity and its gradient on the wedge and the airfoil are the same at the given location. This is covered in AIR1168/2, 3.5.2 and also in Reference 11.

Turbulent heat transfer coefficients are computed from flat plate theory, using the local velocity. For air at normal temperature,

$$\text{Turbulent } h_o = 0.51 (T_m)^{0.3} \cdot \frac{[1.69 \rho_o v]^{0.8}}{s^{0.2}} \quad \text{(Eq. 8)}$$

Transition from laminar to turbulent flow is dependent upon local pressure gradients, local Reynolds number, and local surface roughness that may be a result of ice formation. In the absence of strong pressure gradients, transition will start where the local surface Reynolds number $N_{(Re,s)}$ is 0.5 x 10^6 and will end at $N_{(Re,s)}$ = 2.0 x 10^6. A strong favorable pressure gradient (decreasing static pressure with increasing distance from the leading edge) will delay transition.

Conversely, an unfavorable pressure gradient (increasing static pressure with increasing distance) will promote transition. Impingement limits have no apparent effect on transition for an anti-iced surface.

4.2.1.2 Average

The average external heat transfer curves are based on the assumption of fully turbulent flat plate flow. Owing to this simplified treatment, it is not possible to take into account the effect of airfoil camber or angle of attack. It is probable, however, that such effects fall within the accuracy of the formula used.

The equation for the average heat transfer coefficient over a distance L_x from the leading edge is

$$\text{Average } h_o = 0.64(T_m)^{0.3} \cdot \frac{[1.69\,\rho_o v]^{0.8}}{L_x^{0.2}} \qquad \text{(Eq. 9)}$$

Taking the area per foot of span per surface, i.e., $L_x(1) = S_o$, and putting in the equation of state, Equation 9 becomes (for $T_m = 520$ °R),

$$h_o S_o = 6.32[\rho_o v L_x]^{0.8} \qquad \text{(Eq. 10)}$$

Although h_o is a function of T_{amb}, the change in h_o over the range of ambient temperatures for which icing can occur can be neglected. Hence, $h_o S_o$ may be plotted as a function of v and L_x for various altitudes (for $T_{amb} = 460$ °R) as presented in Figure 11.

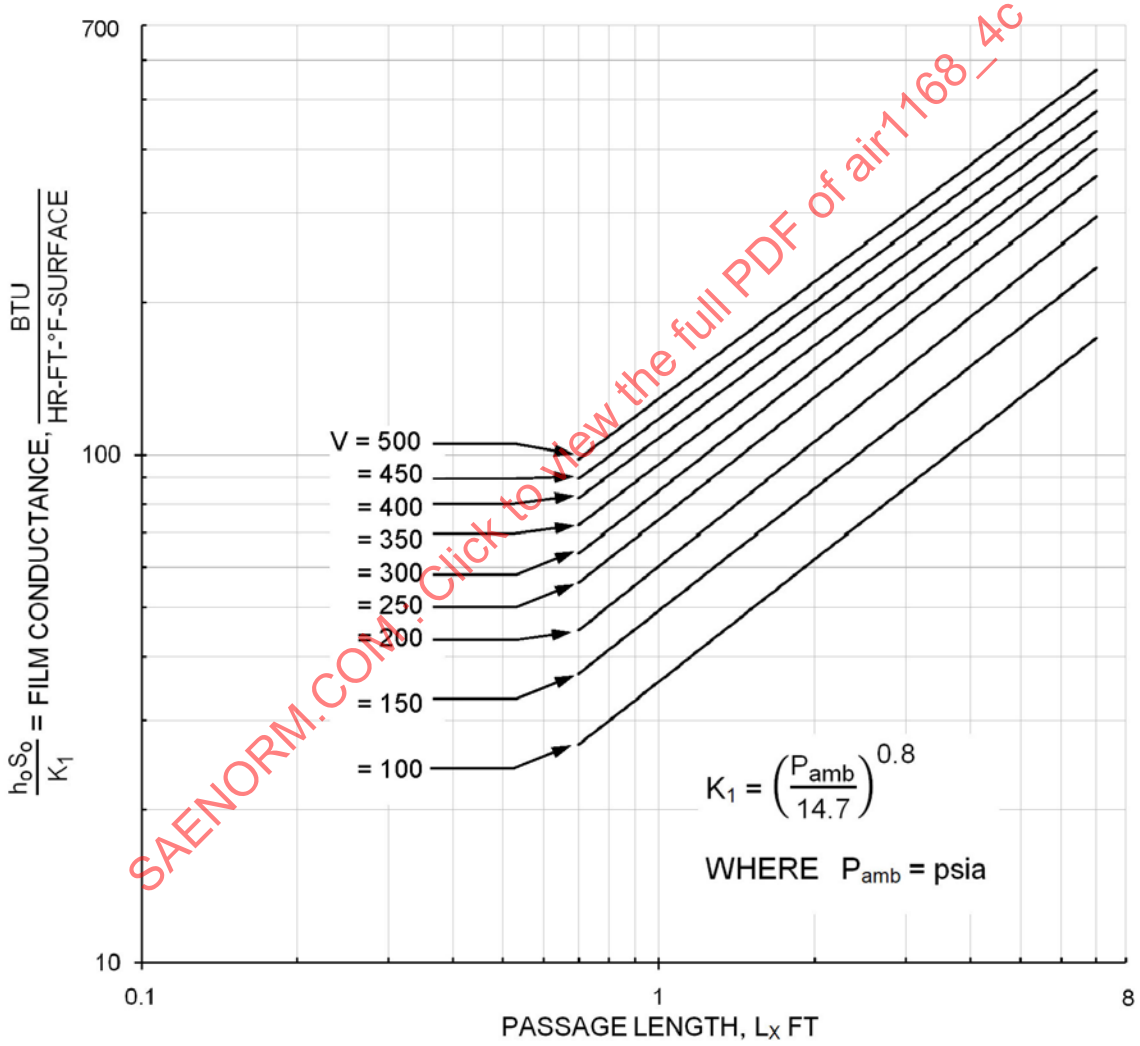

Figure 11 - Average external film conductance for fully turbulent flow over airfoils (v = velocity, knots TAS)

4.2.2 Bodies of Revolution

Figures 12 and 13 (taken from Reference 9) present curves for the determination of local laminar and turbulent heat transfer coefficients over cones. Transition from laminar to turbulent flow may be assumed to occur at

$$\left(N_{(Re,o)}\right)\left(\frac{s}{L_x}\right)\cos\Phi_o = 1.5\times10^6 \qquad \text{(Eq. 11)}$$

where $N_{(Re,o)}$ is based upon freestream conditions and body length. Heat transfer coefficients over ellipsoids can be obtained from Reference 9. For Figures 12 and 13,

$$N_{Nu} = \frac{h_o L_x}{k_o} \text{ and } N_{(Re,o)} = \frac{1.69\rho_o v L_x}{\mu_o} \qquad \text{(Eq. 12)}$$

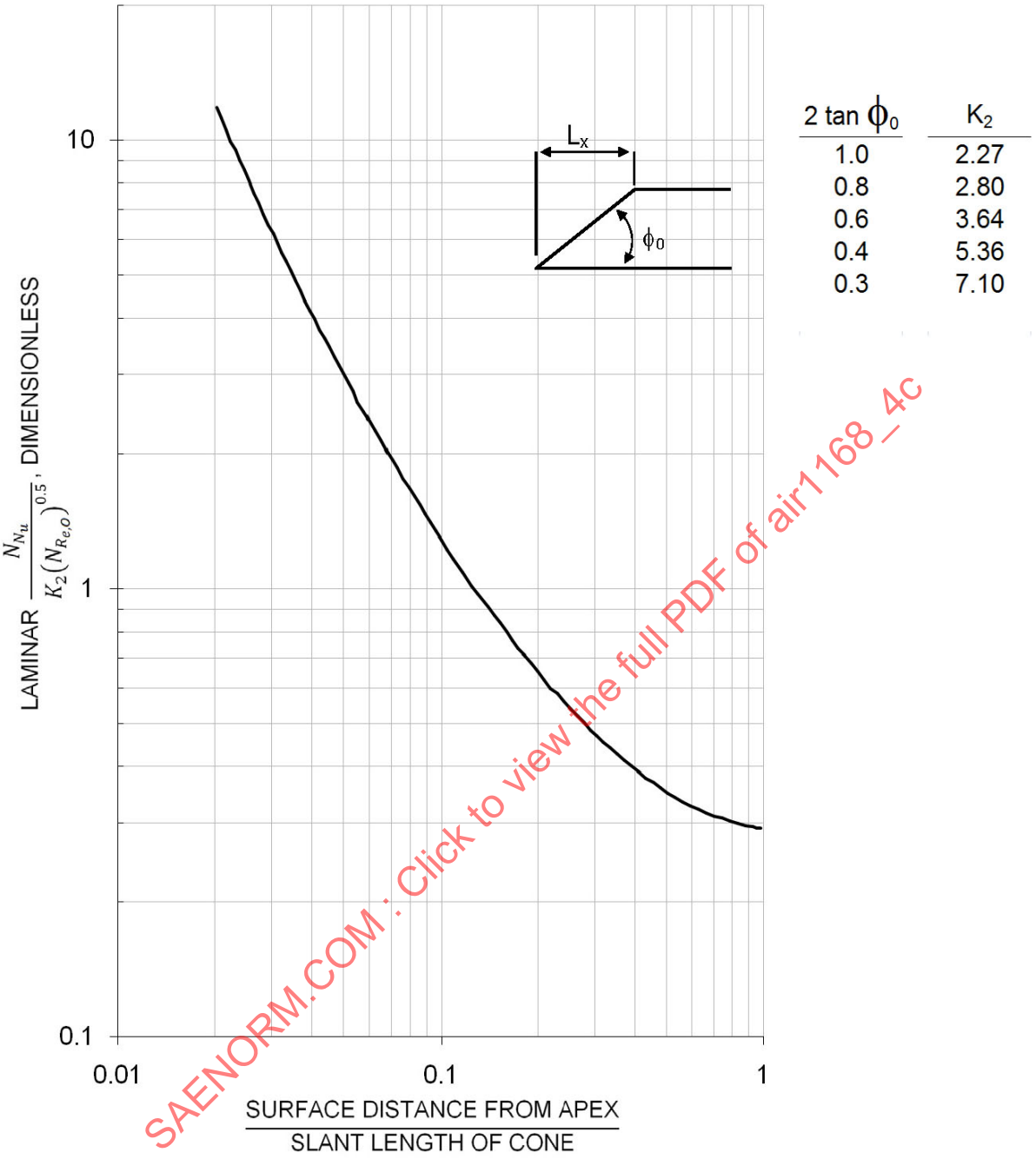

Figure 12 - Laminar heat transfer coefficients over cones

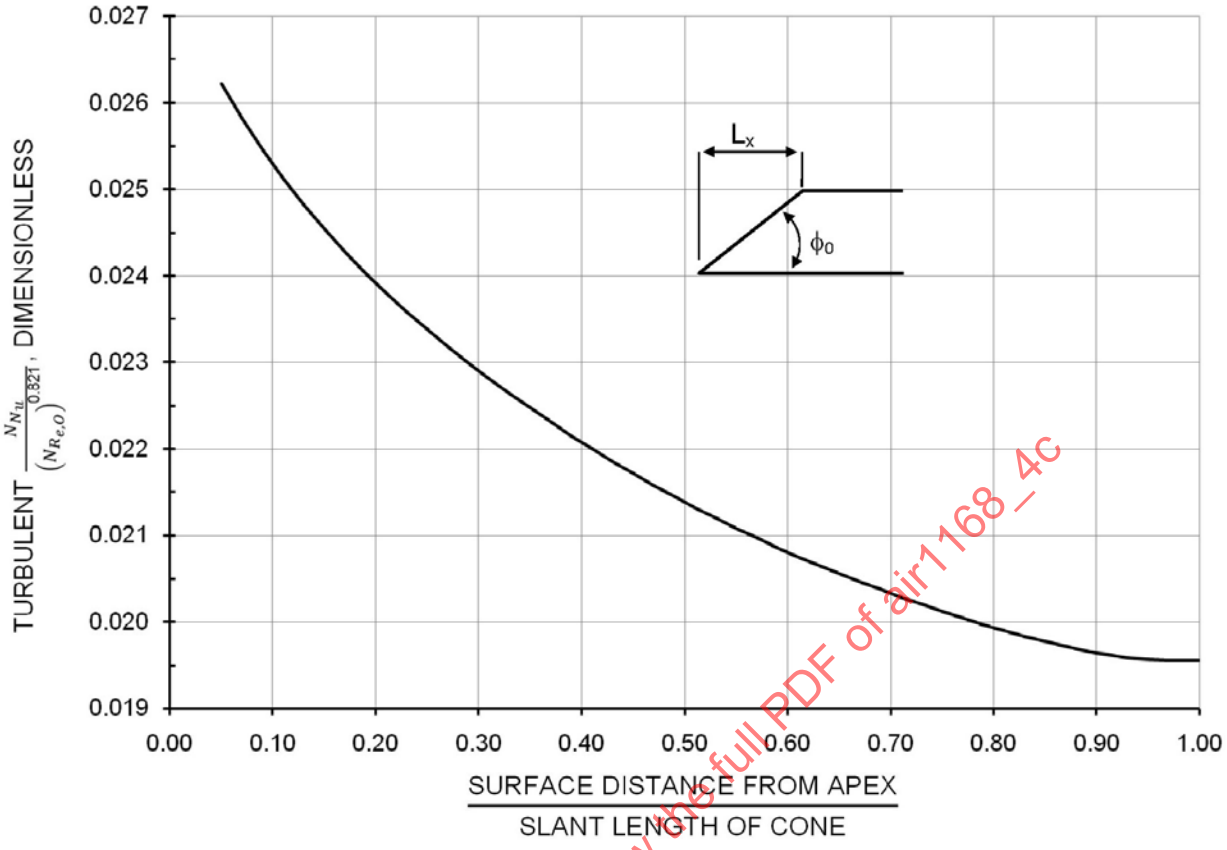

Figure 13 - Turbulent heat transfer coefficients over cones

5. AIRFOIL EVAPORATIVE ANTI-ICING

5.1 Wet Surface Temperature

5.1.1 Wettedness Factor

Wettedness factor, F, is a measure of the surface area over which evaporation occurs, and is related to the impingement limit. Forward of the impingement limit, the water (on a heated surface) tends to form a solid film, and the wettedness factor is unity. Aft of the impingement limit the water flows in rivulets and the wettedness factor F is taken as 0.2. Consequently, the overall wettedness factor could vary from 0.2 to 1.0, depending upon the ratio of impingement limit to heated chord. However, an overall value of 0.6 can be used for computing air flow requirements.

5.1.2 Evaporation Rate

For evaporative anti-icing, the rate of evaporation is equal to the rate of water catch, or

$$M = \frac{2.9 h_o S_o F (p_{sk} - p_w)}{P_{amb} - p_{sk}} \qquad \text{(Eq. 13)}$$

Rearranging Equation 13 and putting in F = 0.6,

$$\frac{M}{h_o S_o} = 1.74 \frac{p_{sk} - p_w}{P_{amb} - p_{sk}} \qquad \text{(Eq. 14)}$$

If $p_{sk} >> p_w$, and since p_{sk} is a function of skin temperature only, then it is possible to plot required skin temperature as a function of M/h_oS_o for various altitudes, as is presented in Figure 14.

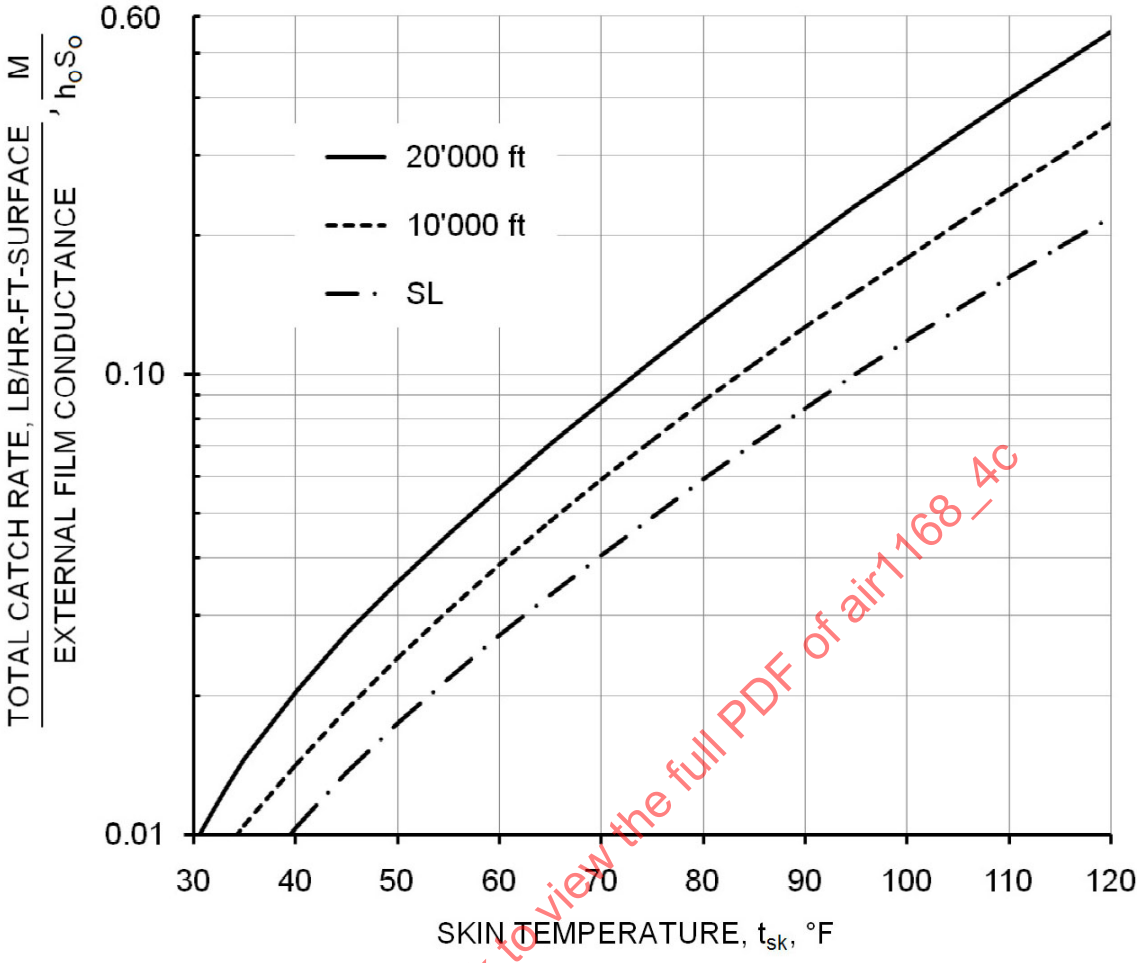

Figure 14 - Skin temperature required for evaporative anti-icing

5.2 Anti-Icing Heat Load

The requirements of a hot air evaporative anti-icing system are determined by the rate at which heat must be supplied to balance the heat losses from the protected surface, which result from three concurrent processes: convective cooling, evaporation, and sensible heating (heating of the impinging water to the skin temperature). The heat load equation is

$$\frac{q}{h_o S_o} = (t_{sk} - t_{aw}) + \left[\frac{M}{h_o S_o} c_w (t_{sk} - t_w)\right] + \left(\frac{M}{h_o S_o} L_e\right) \quad \text{(Eq. 15)}$$

convection sensible heat evaporation

Using a constant value of L_e of 1060 Btu/lb, and rearranging terms,

$$\frac{q}{h_o S_o} = (t_{sk} - t_{aw}) + \frac{M}{h_o S_o} \cdot [L_e + c_w (t_{sk} - t_w)] \quad \text{(Eq. 16)}$$

Since $(t_{sk}-t_w) << L_e$, the difference between t_w and t_{aw} can be neglected, and hence it is possible to plot q/h_oS_o against $(t_{sk}-t_{aw})$ for various values of M/h_oS_o, as shown in Figure 15.

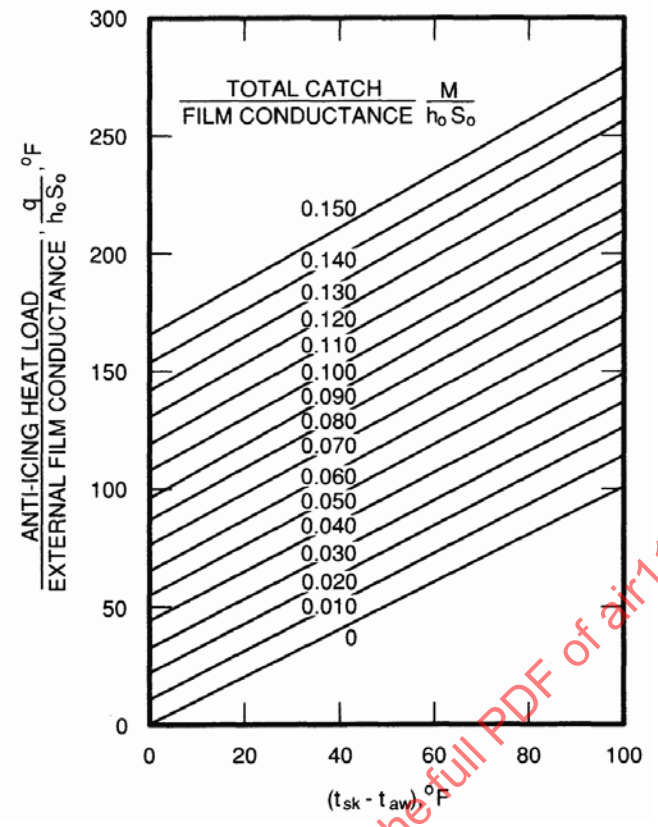

Figure 15 - Airfoil evaporative anti-icing energy requirements

5.3 Determination of Air Flow Requirements

5.3.1 Passage Design

Hot air passages are the corrugated double skin and the machined skin. In the former a second, or inner, skin forms the heat transfer passages as shown in Figure 16A. In the machined skin, chordwise slots are milled in the leading edge and a second flat sheet is used to back up the passages, as shown in Figure 16B. This construction is used where very shallow passages (≈0.05 inch deep) are desired.

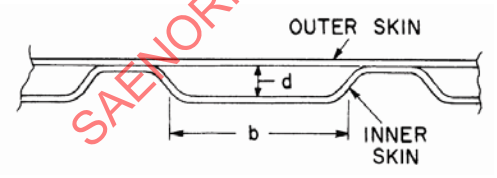

Figure 16A - Corrugated double skin

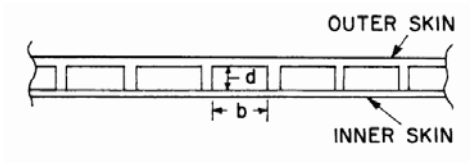

Figure 16B - Machined skin

Figure 16 - Typical passage designs

5.3.2 Internal Heat Transfer Coefficient

The internal heat transfer coefficient for turbulent flow in a passage is

$$h_i = 5.4 \times 10^{-4} \left(\frac{T_m^{0.3}}{D_h^{0.2}} \right) \left(\frac{w_{pa}}{A_{pa}} \right)^{0.8} \quad \text{(Eq. 17)}$$

From Figure 16,

$$A_{pa} = nbd \quad \text{(Eq. 18)}$$

$$D_h = 2\left(\frac{bd}{b+d} \right) = 2\left(\frac{d}{1+(d/b)} \right)$$

Also, we can define the correction factor for passage aspect ratio:

$$Z = \left(1 + \frac{d}{b} \right)^{0.2} \quad \text{(Eq. 19)}$$

Combining these equations,

$$h_i = 5.4 \times 10^{-4} \left(\frac{T_m^{0.3}}{(2d)^{0.2}} \right) \left(\frac{Z}{(bd)^{0.8}} \right) \left(\frac{w_{pa}}{n} \right)^{0.8} \quad \text{(Eq. 20)}$$

5.3.3 Passage Heat Balance

The energy required to satisfy the requirements of Equation 16 is supplied by the enthalpy drop of the passage air, or

$$q = w_{pa} c_p (t_{in} - t_{ex}) \quad \text{(Eq. 21)}$$

The air temperatures are related to the skin temperature by Equation 22:

$$\frac{t_{ex} - t_{sk}}{t_{in} - t_{sk}} = e \exp\left(- \frac{h_i nbYL_x}{w_{pa} c_p} \right) \quad \text{(Eq. 22)}$$

The factor Y in Equation 22 is the correction for passage fin effect brought about by conduction from the inner skin, which effectively increases the internal heat transfer area. The determination of Y is discussed in detail in Reference 34. In the case of a corrugated aluminum passage, Y is approximately 1.6. Insertion of Equation 20 into Equation 22 leads, after considerable rearrangement, to (for $T_m \approx 660$ °R)

$$\frac{q}{nb(t_{in} - t_{sk})} = 0.24 \left(\frac{w_{pa}}{nb} \right) \left\{ 1 - e \exp\left(-0.0137 \frac{L_{eq}}{d} \left(\frac{nb}{w_{pa}} \right)^{0.2} \right) \right\} \quad \text{(Eq. 23)}$$

where $L_{eq} = L_x YZ$ and is defined as the "equivalent passage length." In Figure 17, $q/nb(t_{in}-t_{sk})$ has been plotted as a function of w_{pa}/nb for values of L_{eq}/d. Values of Z are shown as a function of d/b in Figure 18.

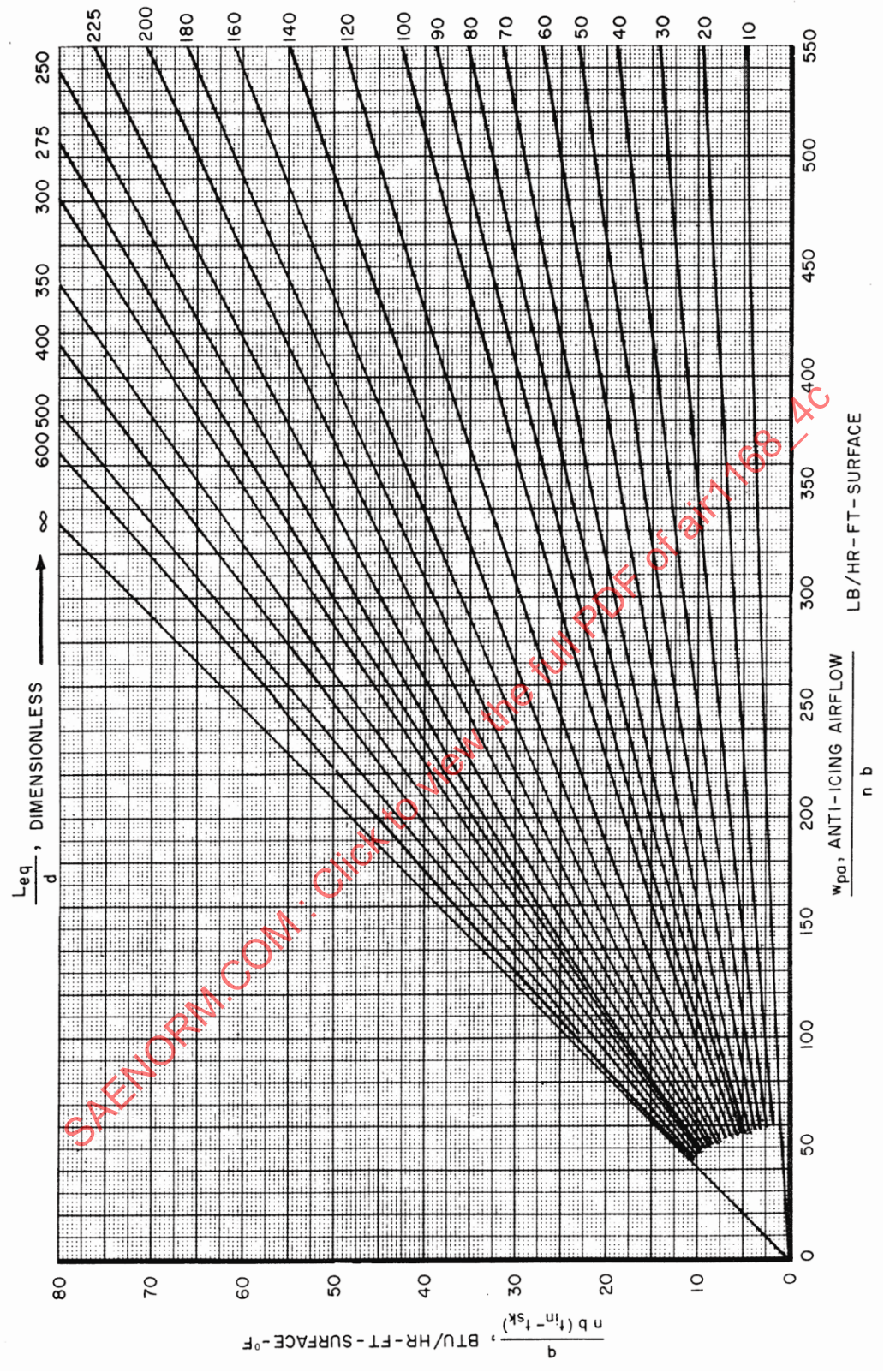

Figure 17 - Air flow required for evaporative anti-icing

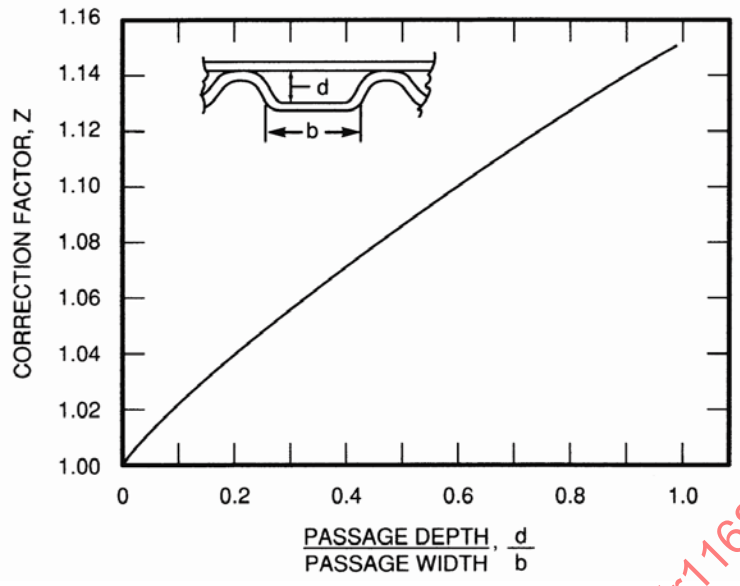

Figure 18 - Correction factor for passage aspect ratio, $Z = (1+d/b)^{0.2}$

5.3.4 Piccolo Tubes

5.3.4.1 Piccolo Tube Design

Another form of leading edge heat exchanger utilized is the piccolo tube (a tube with holes spaced along its length to distribute heated air along the heated surface). See Figure 19.

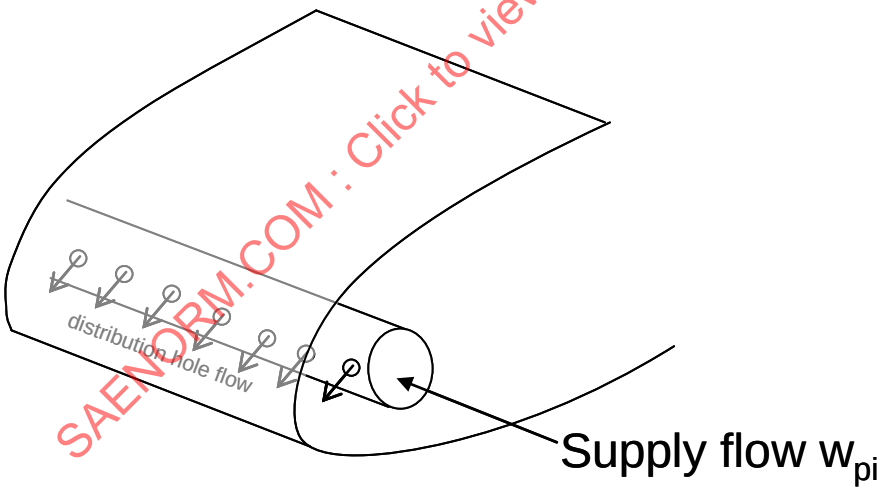

Figure 19 - Piccolo tube in a leading edge

The energy required to satisfy the evaporative heat requirements of Equation 15 or the running wet heat requirements of Equation 21 is supplied by the enthalpy drop of the supplied, heated air, or

$$q = w_{pi} * F_{surface} * c_p * (t_{in} - t_{ex}) \quad \text{(Eq. 24)}$$

Note that some fraction of the supplied flow goes to the “upper” surface in Figure 20, and some to the lower surface. The fraction of the flow that goes to each surface may be manipulated by the placement of the piccolo tube and the aiming of the distribution holes. The protection requirements may differ for the two surfaces (for example, one may require fully evaporative protection, and one may be allowed to run wet), so the desired flow split may not be 50% to each surface. The total flow required is the sum of the flow for the two surfaces.

This analysis method applies best when the distribution holes are aimed near the stagnation line, so that the “upper” and “lower” surface are coincident both with the internal and external heat transfer. This provides maximum heating near the area of maximum local water catch. When this is not the case, as in Figure 20, the analysis is more complex, as the external impingement surface water flow on the “upper” surface as defined by the stagnation line crosses part of the “lower” surface as defined by the internal flow split. A conservative analysis of the upper surface anti-ice performance may be accomplished by assuming the heat contributed by the lower path of the internal, heated flow is negligible. Alternatively, a more complex, two dimensional analysis may be conducted using methods like those in Reference 38.

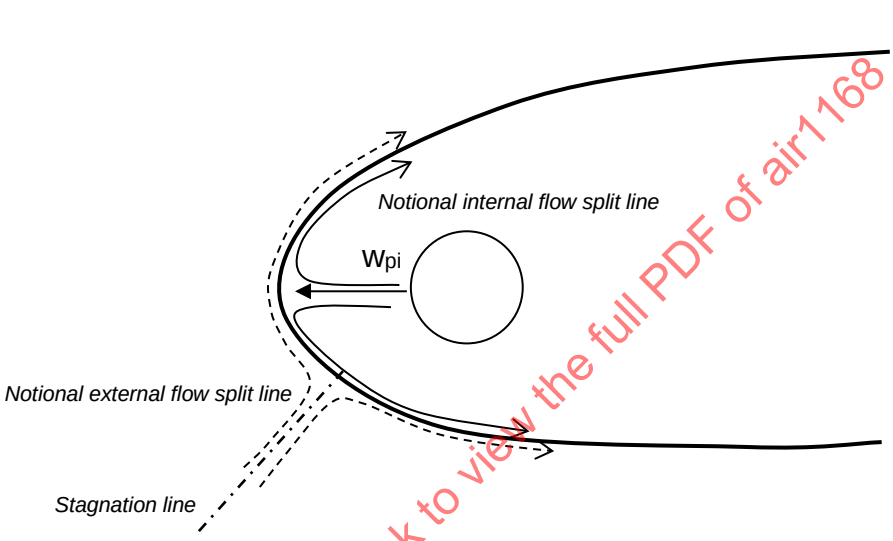

Figure 20 - Flow split on a heated airfoil leading edge

The exhaust temperature is typically determined by test. Dry air tests (in flight or wind tunnel) are sometimes used to determine this temperature. Typical piccolo tube designs achieve a thermal effectiveness (ε, defined below) of at least 40%. It should be noted that the exhaust temperature is expected to be lower in icing conditions than in dry air conditions at the same airspeed and temperature, as there are additional modes of cooling on the outer surface (sensible cooling and evaporation due to impinging drops), which makes the piccolo tube a more effective heat exchanger. Therefore, a heat available calculation based on exhaust temperatures measured in dry air is conservative in that heat available in icing is underestimated.

$$\varepsilon = \frac{t_{in} - t_{ex}}{t_{in} - t_{aw}} \qquad \text{(Eq. 25)}$$

Once the flow requirements are established, the pressure drop of flow along the piccolo tube should be analyzed to verify that there is adequate heating uniformity along the heated span. Piccolo distribution hole size and spacing are selected so that the required flow rate per unit span is achieved at the design point supply pressure and temperature. Manufacturers typically have proprietary methods of selecting the hole sizing and spacing (and distance from the heated surface) to optimize heating efficiency.

The exhaust air typically flows through dedicated exhaust holes in designed locations. Exhaust air should be in a location that minimizes the effect on aerodynamic performance. The exhaust air may be at temperatures high enough that specialized structure is required near the exhaust.

5.3.4.2 Spray Tube Effectiveness Analysis

The typical arrangement of a piccolo tube may be approximated as a parallel flow heat exchanger with a capacity ratio of zero (the external ambient flow acts as an infinite heat sink). While the piccolo flow is typically initially directed forward, counter to the ambient flow, the heat exchange takes place once the flow has turned along the heated surface interior, substantially in the same direction (parallel) to the external flow (the effect of wing sweep is minor for this thermal analysis). The methods of AIR1168/6 may be used to analyze the heat exchanger in dry air conditions.

The piccolo heat exchanger is typically without fins (unlike the examples in AIR1168/6), so internal heated area is approximately the external area, and the UA value may be calculated using AIR1168/6 Equation 3H-112 with the areas set equal to one another and the fin effectiveness set at unity:

$$\frac{1}{U_{ov}A} = \frac{1}{A_h U_h} + \frac{thick}{A_w k} + \frac{1}{A_c h_c} = \frac{1}{A} * \left(\frac{1}{h_o} + \frac{thick}{k} + \frac{1}{h_i} \right) \quad \text{(Eq. 26)}$$

The NTU value may be calculated from AIR1168/6, Equation 3H-107:

$$NTU = \frac{U_{ov}A}{C_{min}} \quad \text{(Eq. 27)}$$

The thermal effectiveness is then calculated (from AIR1168/6 Equations 3H-106 and 3H-118):

$$\varepsilon = \frac{t_{in} - t_{ex}}{t_{hi} - t_{aw}} \approx 1 - e^{-NTU} \quad \text{(Eq. 28)}$$

Reference 37 describes various correlations used to calculate the internal heat transfer coefficient. More recently, computer code methods have been used (also described in Reference 37).

For icing conditions, an “effective” external heat transfer coefficient may be used in place of the dry air external heat transfer coefficient:

$$h_{o,eff} = \frac{q/S}{(t_{sk} - t_{aw})} \quad \text{(Eq. 29)}$$

The equation may be divided into heat transfer modes, similar to those from Equation 15

$$h_{o,eff} = \frac{q/S}{(t_{sk} - t_{aw})} = \frac{q_{convection}/S}{(t_{sk} - t_{aw})} + \frac{q_{sensible}/S}{(t_{sk} - t_{aw})} + \frac{q_{evaporation}/S}{(t_{sk} - t_{aw})} \quad \text{(Eq. 30)}$$

The first term corresponds to the dry air convective heat transfer, and the other terms are the additional modes of heat transfer in icing conditions.

5.3.4.3 Note that the effective external heat transfer coefficient value calculated for icing conditions is sensitive to the heat supplied and surface temperature, and is used in the calculation of heat supplied and surface temperature, so an iterative solution is required. Additional piccolo tube analyses are contained in References 42 through 56.

6. RUNNING WET ANTI-ICING

Energy requirements for running wet anti-icing are found by combining Equations 13 and 15 and setting F = 1.0, or

$$\frac{q}{h_o S} = (t_{sk} - t_{aw}) + \frac{M_\beta}{h_o} c_w (t_{sk} - t_w) + \frac{2.9 L_e (p_{sk} - p_w)}{P_{amb} - p_{sk}} \quad \text{(Eq. 31)}$$

The choice of unity wettedness factor results from the assumption of a solid film of water over the entire heated area. The use of this equation differs from that of the preceding section in that a desired skin temperature (35 to 50 °F) is selected beforehand and the energy requirements computed directly.

Another difference is that, whereas evaporative anti-icing requirements were based upon average quantities, running wet anti-icing requirements are computed using the local values of water catch rate and heat transfer coefficients. Figure 21 shows q/h_oS plotted against velocity and M_β/h_o for a skin temperature of 40 °F (a conservative value) and an ambient temperature of 0 °F (specification requirement).

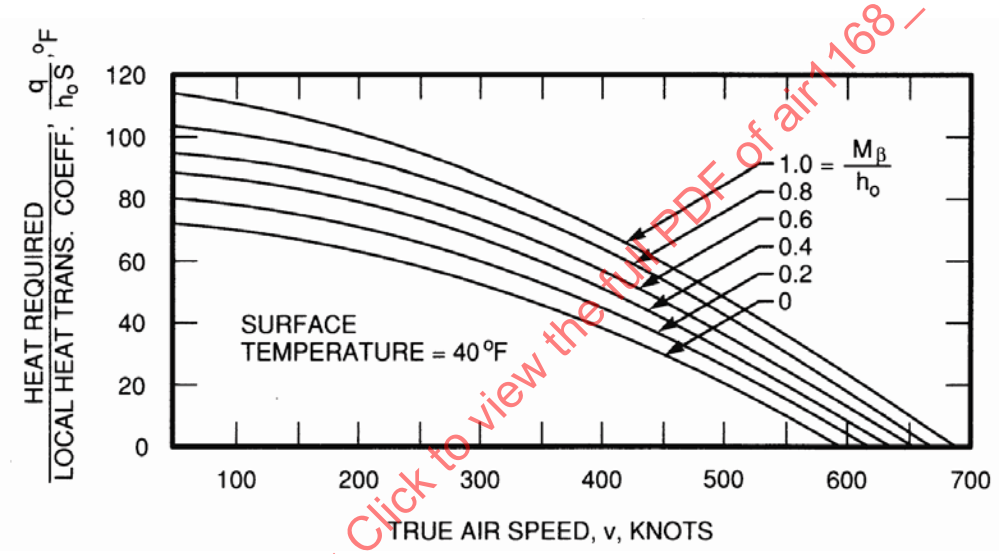

Figure 21 - Energy requirements for running wet anti-icing. Surface temperature = 40 °F, 10000 feet at 0 °F ambient. To obtain values for other altitudes: subtract 11.0 for sea level, add 15.0 for 22000 feet

The values in Figure 21 assume 100% heating efficiency; that is, no heat loss to the structure. Heating efficiency normally varies from 60 to 100%, depending upon the type of construction, proximity of unheated areas, and similar factors. Because of the varying requirements from point to point, running wet anti-icing lends itself to the use of electrical resistance elements for the energy supply. In this case, heating efficiency may be taken as 70% along the edge of the heated area, and may be increased roughly exponentially to unity at approximately 8 inches in from the edge.

7. ELECTROTHERMAL CYCLIC DEICING

7.1 Description

Electrothermal deicing technology has been the state of the art system for many years on helicopter or turboprop blades. Design considerations for rotor blade electrothermal ice protection have been published in Reference 17 and will not be discussed herein except for clarification.

With the development of lightweight AC electrical systems, electrothermal deicing has found many applications on new aircraft designs as a power conservation measure. The leading edge area to be protected is divided into several spanwise and chordwise areas, with each area energized sequentially or, at most, with corresponding areas on opposite sides of the airplane energized simultaneously. A possible heater layout for a half wing is shown in Figure 22.

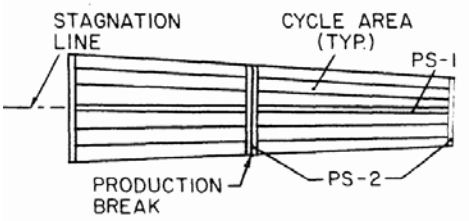

Figure 22 - Half wing heater layout

For slightly swept airfoils, a 1 inch-wide, heated parting strip (PS-1) is provided along the stagnation line to prevent ice from bridging over between the top and bottom surfaces and to allow aerodynamic forces to remove the ice. The width of the parting strip suggested may vary based on airfoil geometry, running wet or evaporative system and the ice accumulation allowed to form on the deicing zones aft of the parting strip. Tiltrotor and turboprop aircraft may use the parting strip to minimize the size of ice shed from the blade deicing zones onto the fuselage and therefore may not locate the parting strip at the stagnation line. In addition, 3/4 inch-wide chordwise parting strips (PS-2) should be added adjacent to the unprotected areas and on either side of production breaks.

The deicing cycled area may be divided into multiple chordwise areas, the cycling sequence being from front to rear or tip to root for spanwise deicing system (Reference 35). Sometimes the rearmost element is aft of the impingement limits to clear off any runback ice (formed while the recently shed areas are still above freezing and the impinging water merely runs back along the surface).

On highly swept airfoils, the spanwise parting strip (PS-1) may not be necessary because the spanwise components of the aerodynamic forces may be sufficient to cause the ice to shed spanwise. Under these circumstances, only one chordwise shedding area need be employed, with the farthest edge area being shed first.

7.2 Heater Construction

Note that deicing may not be the appropriate mode of protection if damage from the shedding process is expected, such as for aft mounted engines. In these cases, anti-icing may be more appropriate.

The basic heater construction consists of electrical resistance elements sandwiched between two layers of dielectric material, with some form of rain and hail resistant material applied to the external surface. Additionally, a safe path for lightning energy dissipation should be provided. Heaters for military application should also be tolerant of ballistic damages. Heater deicing performance is measured in terms of a deicing efficiency, which is defined as the heat leaving the surface integrated over the "ON" time divided by the total heat input. Deicing efficiency is, in turn, influenced by the heater construction, typical values ranging from 20 to 40% for various designs. Heater deicing efficiency is reduced by improper heater design in several ways:

1. Not all the heat input goes out the external surface; some of it goes back into the leading edge skin, plenum areas and attachment structures.

2. The heater itself absorbs heat while being heated up to the temperature required for deicing.

3. Normally heater resistance will increase with heater temperature and therefore produce less power.

4. Discrete heater elements, such as ribbons or wires, result in nonuniform heating of the external surface, and thus power inputs must be increased to ensure that the areas between the heater elements are sufficiently heated.

5. Construction may have local discrepancies in terms of material thickness and thermal conductivity.

6. Manufacturing tolerance may impact heater resistance and may create local resistance changes due to heater bends.

The optimum heater buildup is one that maximizes deicing efficiency and at the same time is light in weight and has good rain and hail resistance. While obtaining a light weight heater is a design goal, the total system weight must also be considered. This is especially true for protected surfaces that may have ice accumulation characteristics that differ from a 2D airfoil due to spanwise wing sweep, certain empennage design features, etc.

Some heater designs utilize glass cloth impregnated with epoxy or phenolic resins as the dielectric material. Erosion resistance is provided by a sheet of metal. Thickness of material and selected material vary greatly with specific application and erosion protection methods. This design also helps improve the uniformity of heat distribution and adds some rigidity to the sandwich, thus potentially reducing the leading edge skin thickness. A cross section of this type of construction is shown in Figure 23.

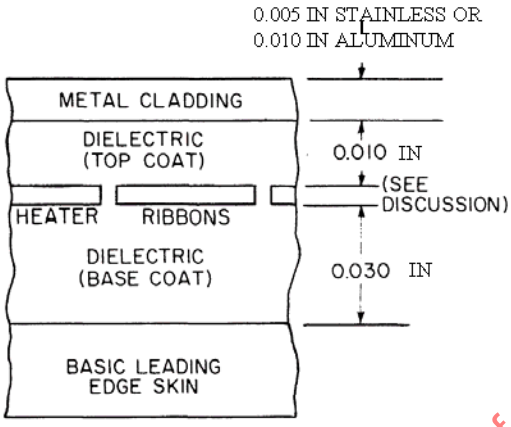

Figure 23 - Example heater construction

Heater ribbon thickness varies with the material used, ribbon width, and desired resistance. The thickness is typically 0.003 to 0.005 inch. Although the metal cladding will help spread the heat, the heater ribbon should be at least five and preferably ten times as wide as the allowable gap between ribbons, to ensure uniform surface temperature. With a maximum gap width of 0.05 inch, this means a ribbon width of 0.25 to 0.5 inch. The ratio of base coat to top coat thickness of 3:1 has been found to be a good compromise between heater efficiency and heater weight. For this particular construction the deicing efficiency is approximately 40%.

Rotorcraft and some Turboprop blade heaters use braided wires. Braided wire heaters are one of the few current technologies that can cope with high strain level over the expected life of such blades. This type of environment causes the design of such a heater to be very specific and is not expected to meet the suggested dimensions above.

The uniform layers of graphite and other types of conductive materials have been used as an alternate to braided wires or metal ribbon.

7.3 Parting Strip Power Requirements

Parting strip power requirements are computed in much the same manner as those for anti-icing (Section 5 or 6). The basic difference is that the presence of ice layers on the adjacent cycled areas slightly affects parting strip power requirements while adjacent zones are energized and have almost no effect when they are not energized. Because of conduction into the cycled areas, a surface temperature of 50 °F at the center of the parting strip is necessary to ensure a finite ice-free area and prevent adjacent ice formations combined with runback refreeze from the running wet condition from bridging over. Generally, 12 W/in^2 (5900 Btu/h-ft^2) will suffice for a 0 °F ambient, while 20 W/in^2 (9800 Btu/h-ft^2) are required for a -22 °F ambient. These values are approximate and depend on the heater construction, geometry and operational conditions. In particular, thicker skins and cladding or thinner base coats may increase the power requirements by 10 to 20%. Consequently, the actual powers used should be verified by tests.

The heater and adjacent material layers' maximum temperature should be verified to not exceed limits and cause structural damage to the construction for non-icing condition in ambient temperature when the system could reasonably be operated.

Expected surface temperature should be obtained in a reasonable amount of time. Warmup time and recognition time should be considered in determining preactivation ice shapes. Times between 30 seconds to 2 minutes have typically been used, including recognition of icing conditions and activation of the system.

7.4 Cyclic Requirements

Cyclic requirements are a function of impingement limits, power available, and total cycle time (number of elements times the "ON" time for each element). The required power intensity is primarily a function of the unheated equilibrium temperature (8.3) and the heat-on time; the heat-off time, ice thickness, catch rate, and heat transfer coefficient have second order effects.

For the most efficient removal of ice, minimum runback ice, and minimum total energy input, high power intensities for very short periods give the best results. However, for a given total power available, this results in a large number of elements and the consequent increase in weight and timer complexity. Additionally, this also increases the severity of construction damage in the event of improper operation.

As a compromise, reduced power input for longer durations can be used to obtain good deicing performance. For total cycle time, one to three minutes has been used as a compromise for total power requirements (the more elements, the lower the total power), with the performance loss occurring during the heat-off period. Since heater construction plays a major role in deicing performance, the final design should be verified by tests.

8. DETERMINATION OF THE NEED FOR ICE PROTECTION

8.1 Design Point

Regardless of the type of ice protection employed (evaporative, running wet or cyclic), it is necessary to design the system to meet the severest icing condition the airplane is anticipated to encounter. This is determined by superimposing the airplane mission on the applicable government requirements (8.2) and computing the energy requirements for several flight conditions. In addition, an envelope should be drawn, using the methods of 8.3, showing the flight conditions for which ice protection is not required because the unheated equilibrium temperature is above freezing. The following paragraphs present some general statements regarding the selection of a design point.

In general, hot air systems, which rely primarily on ram pressure for adequate air flow, must be sized for the highest altitude at which ice is expected, usually 20000 to 22000 feet. Systems employing compressor bleed air must be sized for the lowest engine power settings (in some cases, descent power) because of reduced bleed temperatures, pressures, and available air flow. Generally, the condition of lowest ambient temperature is the most critical, from a heat requirement consideration, but in the case of the civil requirement the increase in required liquid water content with ambient temperature (Figure 24) may more than offset the reduced convective losses.

Since the energy available from electrothermal systems, either running wet or cyclic, is constant, they must be sized for maximum energy requirements. For running wet systems, this usually occurs in the vicinity of 250 to 350 knots true air speed at sea level. At velocities greater than this, the increase in equilibrium temperature due to the kinetic rise offsets the increased convective losses. This is presented only as a guide and should be verified for the particular application.

Since cyclic requirements are primarily a function of unheated equilibrium temperature (7.4), such a system should be designed for the condition where this temperature is a minimum (see Figure 25).

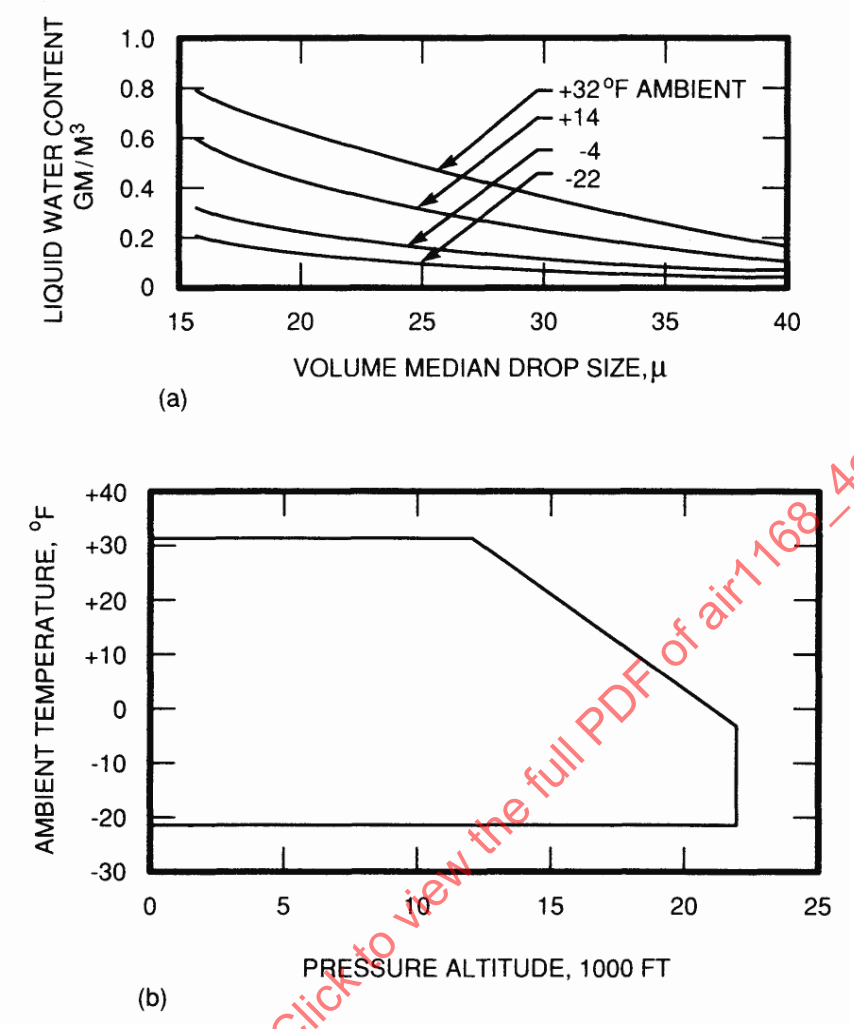

Figure 24 - Continuous maximum icing condition. altitude: sea level to 22000 feet; maximum vertical extent, 6500 feet; horizontal extent, 17.4 nmi. (a) liquid water content, (b) envelope of icing temperature.

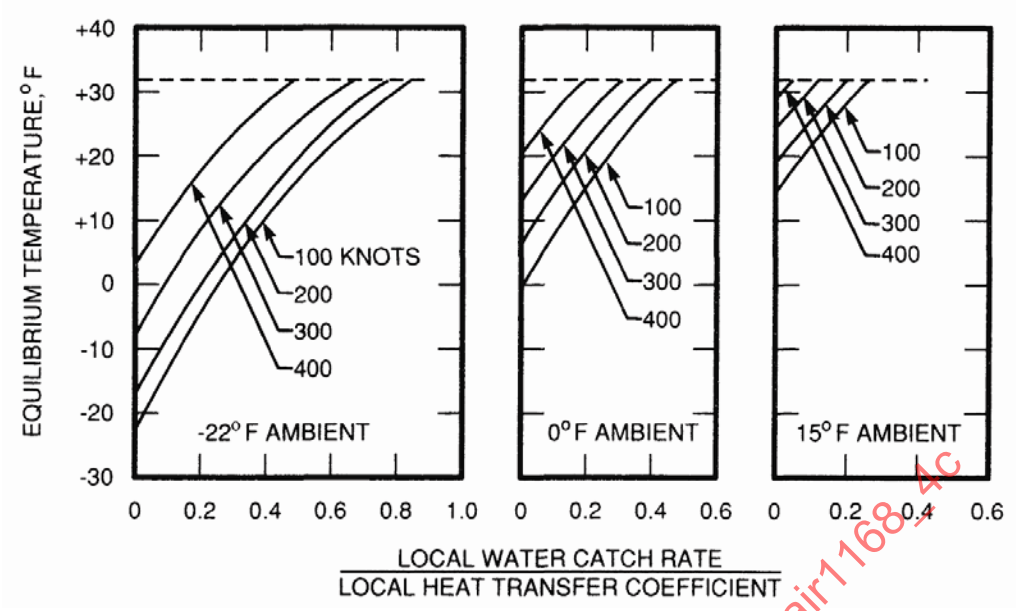

Figure 25 - Unheated equilibrium temperature of an iced surface, all altitudes

8.2 Government Regulations

8.2.1 Commercial Airplanes and Rotorcraft

The ice protection requirements for commercial airplanes and rotorcraft are specified in References 12, 39, 40, and 41 as well as international equivalents not referenced (Transport Canada, EASA, etc.). The icing definitions are applied in a similar manner for both airplanes and rotorcraft, as such the following discussion references transport aircraft requirements per the 14 CFR Part 25 (Reference 12), but is generally applicable to all commercial designs. Two regimes are considered: continuous and intermittent maximums, as defined below and as plotted in Figures 24 and 26 (continuous) and in Figures 26 and 27 (intermittent).

The continuous maximum icing condition (Figures 24 and 26) is characterized by exposure to moderate-to-low liquid water content for an extended period of time. It is applicable to those components such as wing and tail surfaces that are affected by continuous flight in icing conditions but which can tolerate brief and intermittent encounters with conditions of greater severity. The 14 CFR Part 25 does not specify infinite extent, but does specify a standard horizontal extent of 17.4 nmi (Figure 24), with a correction factor to be applied to liquid water content for other ranges (Figure 26).

The intermittent maximum icing condition (Figures 26 and 27) is characterized by exposure to high liquid water contents for a short period, usually superimposed upon the continuous maximum. It is applicable to those components such as engine inlets and guide vanes where ice accretions, even though slight and of short duration, cannot be tolerated. The standard horizontal extent for this condition is 2.6 nmi, as compared with 17.4 nmi for the continuous maximum.

In addition, rulemaking is nearly approved for the consideration of supercooled large drops (freezing drizzle and freezing rain) for commercial transport airplanes 14 CFR Part 25 (Reference 12) and the process is beginning for smaller airplanes within 14 CFR Part 23 (Reference 39). The corresponding environment conditions envelope is proposed to be added as “Appendix O” to 14 CFR Part 25. These conditions should be considered when determining the performance requirements for any thermal protection system. Since the rulemaking is in development at the time of publication of this document, References 12 and 39 and any associated advisory materials should be consulted for consideration of this aspect for ice protection design.

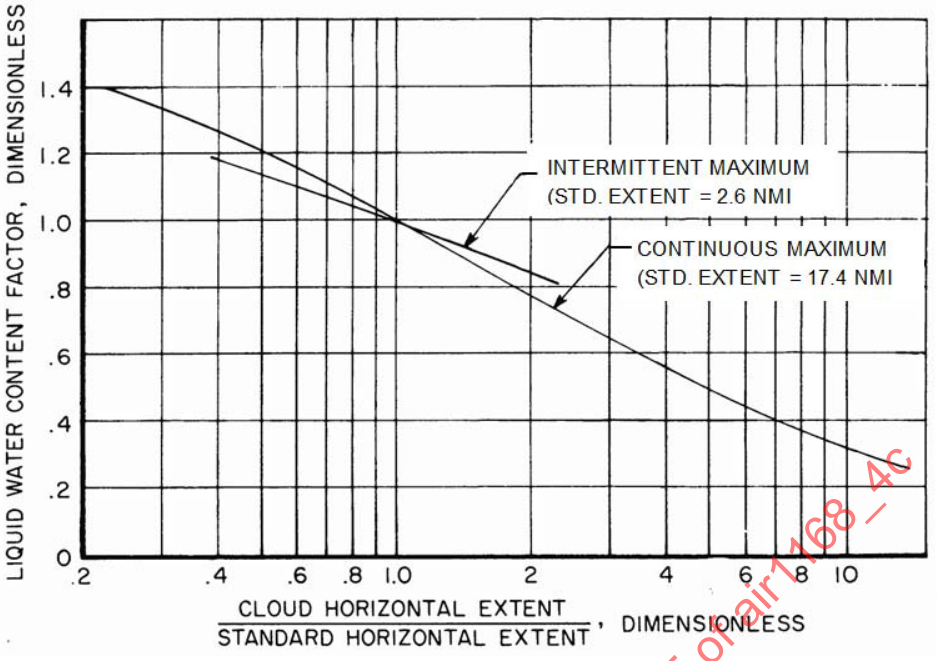

Figure 26 - Variation of liquid water content with cloud horizontal extent

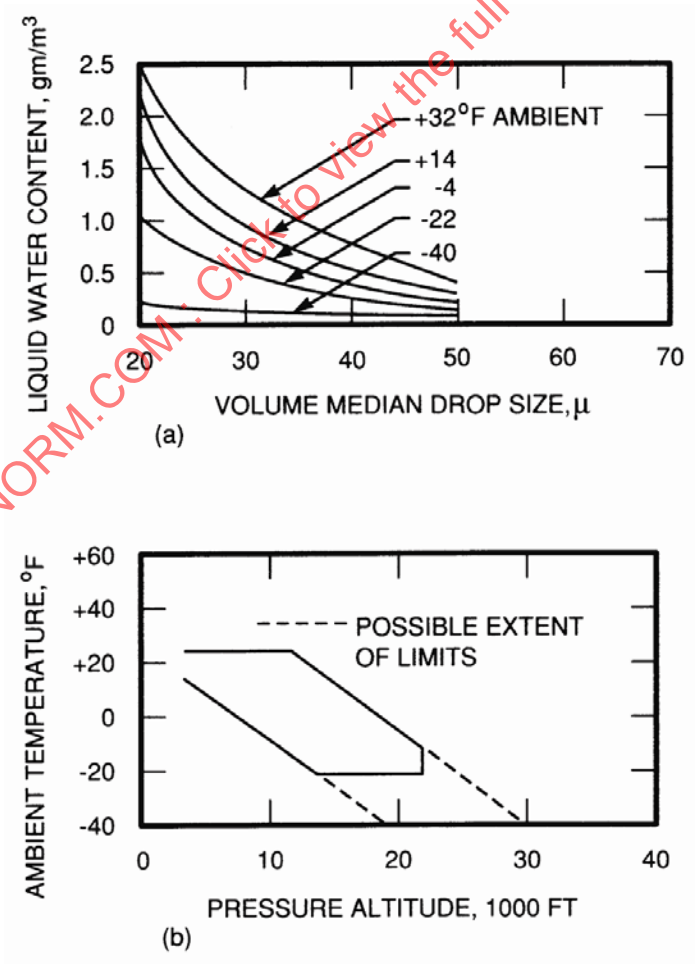

Figure 27 - Intermittent maximum icing condition. Altitude: 4000 to 22000 feet; horizontal extent: 2.6 nmi, (a) liquid water content, (b) envelope of icing temperature

8.2.2 Military Aircraft

The U.S. military now uses performance based specifications in lieu of specifying design requirements, relying on commercial specifications to specify best design practices. Military guidelines for design icing conditions (References 13, 14, and 15) differ in some respects from those of 14 CFR Part 25. Anti-icing guidelines for turbine engines are specified in Reference 14. Guidelines for ice protection of airfoils and other aircraft surfaces are provided in Reference 15. Unlike commercial aircraft, military requirements for the length of time to operate in icing will vary significantly with the mission of the aircraft. This may make a significant difference in the amount of coverage by ice protection systems.

8.3 Unheated Equilibrium Temperature of an Iced Surface

8.3.1 Surface Temperature Below Freezing

The surface of an unheated body flying in an icing condition will assume an equilibrium temperature that just balances convection, sensible heating, and sublimation (Section 5). This temperature may be obtained by setting q/h_oS_o in Equation 15 to zero and replacing the latent heat of evaporation with the latent heat of sublimation (approximately 1220 Btu/lb) to solve for the skin temperature. This leads to the family of curves shown in Figure 25. It must be remembered that these curves apply only to surface temperatures below 32 °F.

8.3.2 Surface Temperature Above Freezing

Of more specific applicability to the question of the need for ice protection are the flight regimes for which the unheated equilibrium is above freezing (Figure 24). For any given icing condition, ice protection is not required for velocities above those shown in Figure 28. The significance of the axis representing zero catch rate is that it indicates for what conditions any runback aft of the impingement area will not freeze. Figure 28 shows that all-weather supersonic aircraft do not need ice protection except during low speed operation (that is, landing, take-off, loiter, etc.) and hence require only limited protection on engine inlets and no protection on wing and tail surfaces.

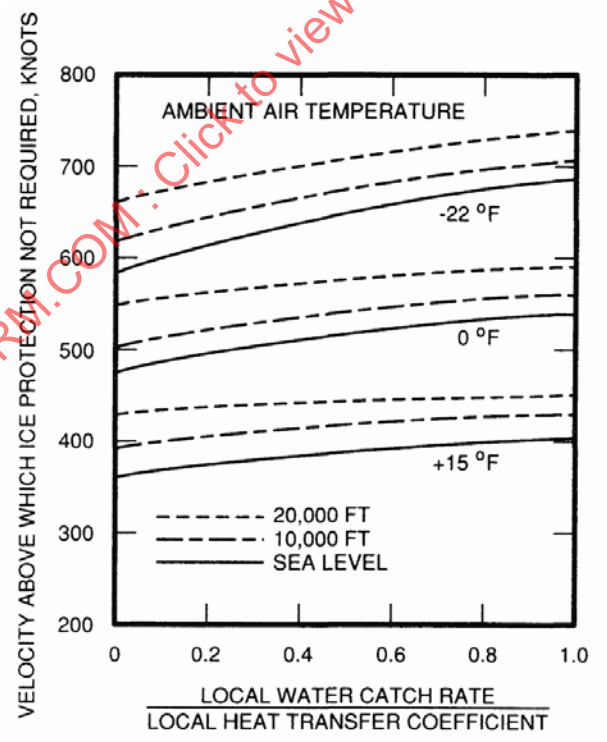

Figure 28 - Velocity above which ice protection is not required

9. ILLUSTRATIVE EXAMPLES

9.1 Airfoil Hot Air Evaporative Anti-Icing

The anti-icing provisions of a commercial transport are to be determined in compliance with the 14 CFR Part 25 for 300 knots true air speed at 20000 feet, with a design icing condition of 20 µm volume median drops and +15 °F ambient air temperature. From Figure 24, the 14 CFR Part 25 continuous maximum requirement is 0.44 g/m^3. The airfoil geometry is listed in Table 1.

Table 1 - Airfoil geometry

Quantity	Value
Airfoil Section	NACA 65_2-015
Chord Length (Mean Aerodynamic)	150 inches
Maximum Thickness	22.5 inches (= 1.87 feet)
Passage Length, L_x	
(for front spar at 19% chord)	27 inches (= 2.25 feet)
Number of Passages per	
ft-span/surface, *n*	4
Passage Width, *b*	2.0 inches
Passage Depth, *d*	0.125 inches

In addition, a passage inlet air temperature of 280 °F will be assumed. Normally, this temperature will have to be determined for the particular installation.

1. Compute passage equivalent length. From the airfoil geometry in Table 1,

$$nb = \frac{4 \times 2.0}{12} = 0.667 \quad \text{(Eq. 32)}$$

$$\frac{d}{b} = \frac{0.125}{2.0} = 0.0625 \quad \text{(Eq. 33)}$$

From Figure 18, Z = 1.014, and hence (from 5.3.3),

$$\frac{L_{eq}}{d} = \frac{(L_x)(Y)(Z)}{d} = \frac{27 \times 1.6 \times 1.014}{0.125} = 350 \quad \text{(Eq. 34)}$$

2. Compute total water catch. From Figure 3,

$$\frac{M}{LWC} = 22.0 \quad \text{(Eq. 35)}$$

$$\text{or } M = \frac{22.0 \times 0.44}{2} = 4.84 \text{ lb/h-ft of span per surface}$$

The factor of 2 in the preceding equation accounts for the split of the water catch about the stagnation point; that is, half the water catch is assumed for each top and bottom surface.

3. Compute external film conductance. From Figure 11, at L_x = 2.25 feet,

$$\frac{h_o S_o}{K_1} = 165 \text{ Btu/h-°F-ft of span per surface} \quad \text{(Eq. 36)}$$

For 20000 feet, K_1 = 0.5365, and therefore:

$$h_o S_o = 165 \times 0.5365 = 88.5 \text{ Btu/h-°F-ft of span per surface}$$

4. Compute required skin temperature. Using data obtained in steps 2 and 3,

$$\frac{M}{h_o S_o} = \frac{4.84}{88.5} = 0.055 \quad \text{(Eq. 37)}$$

From Figure 14, t_{sk} = 59 °F.

5. Compute anti-icing heat load. For 300 knots TAS and +15 °F ambient,

$$t_{aw} = 34 \text{ °F} \quad \text{(Eq. 38)}$$

$$\text{or } (t_{sk} - t_{aw}) = 59 - 34 = 25 \text{ °F}$$

$$\text{From Figure 15, } \frac{q}{h_o S_o} = 86$$

Therefore, q = 86 x 88.5 = 7611 Btu/h-ft of span per surface.

6. Compute anti-icing air flow. Using data obtained in steps 1, 4, and 5,

$$\frac{q}{nb(t_{in} - t_{sk})} = \frac{7611}{(0.667)(280 - 59)} = 51.6 \quad \text{(Eq. 39)}$$

From Figure 17, at L_{eq}/d = 350,

$$\frac{w_{pa}}{nb} = 270 \text{ lb/h-ft of span per surface}$$

and hence the required air flow for both top and bottom surfaces is

270 x 0.667 x 2 = 360 lb/h-ft of span

To obtain the total airplane requirements it is necessary merely to repeat this procedure at several stations and integrate the results.

9.2 Airfoil Hot Air Evaporative Anti-Icing with Piccolo Type Heat Exchanger

The analysis process is similar for a piccolo type heat exchanger and a passage type heat exchanger. The same flight parameters and heated surface length from the previous example for a passage type heat exchanger will be used.

1. Compute heat load

   The heat required for full evaporation on the upper surface is the same as the previous example, = 7611 Btu/h-ft of span per surface

2. Compute anti-icing air flow

   The piccolo heat exchanger will be assumed to have a thermal effectiveness of 0.4:

$$\varepsilon = \frac{t_{in} - t_{ex}}{t_{in} - t_{aw}} \quad \text{(Eq. 40)}$$

   The supply air temperature is assumed to be 280 °F as in the prior example. The adiabatic wall temperature was previously calculated as 34 °F.

$$0.4 = \frac{(280 - t_{ex})}{(280 - 34)} \Rightarrow t_{ex} = 182 \text{ °F}$$

   It is assumed that half of the heating air is directed to the upper surface:

   The total flow required (upper and lower surface) is then calculated:

$$7611 = w_{pi} * 0.5 * 0.24 * (280 - 182) \Rightarrow w_{pi} = 647 \text{ lb/h-ft of span} \quad \text{(Eq. 41)}$$

9.3 Engine Inlet Electrothermal Running Wet Anti-Icing

The engine inlet duct of an all-weather supersonic aircraft is to have a 40 °F running wet surface temperature at a design icing condition of 0.50 g/m^3 of 20 µm volume median drops at 0 °F ambient. The annular inlet has a 2.0 foot long central conical spike having a semivertex angle (Φ_o) of 21.8 degrees. Because of the annular inlet, the cone anti-icing efficiency may be assumed to be unity. The analysis will be performed at a surface distance of 15.0 inches from the apex of the cone.

Selection of a design point for this system requires knowledge of the power requirement as a function of flight speed and altitude. However, for the purpose of illustration, this example will be restricted to 250 knots at sea level.

1. Compute water catch. From Figure 8, at L_x = 2 feet (24.9 inches),

$$E_m = 0.52 \quad \text{(Eq. 42)}$$

   and

$$\frac{\beta_{max}}{\sin \Phi_o} = 0.77 \text{ or } \beta_{max} = 0.286$$

   From Figure 9, s_b/slant length = 0.92; since slant length = $L_x/\cos\Phi_o$,

$$s_b = \frac{0.92 \times 24.0}{\cos 21.8 \text{ deg}} = 23.7 \text{ inches from apex} \quad \text{(Eq. 43)}$$

Using Equation 7,

$$S_m = \frac{(23.7/24.0)^2}{\sin 21.8 \text{ deg}} = 2.62$$

and hence (using Equation 6),

$$\Gamma = \frac{0.52}{(0.286)(2.62) - 0.52} = 2.26$$

For a surface distance s of 15.0 inches,

$$\frac{s}{s_b} = \frac{15.0}{23.7} = 0.623$$

From Figure 9,

$$\frac{\beta}{\beta_{max}} = 0.87$$

and therefore $\beta = 0.248$.

Using Equation 3, the local water catch is

$$M_\beta = 0.38 \times 250 \times 0.50 \times 0.248 = 11.8 \text{ lb/h-ft}^2$$

2. Compute freestream Reynolds number. Freestream air properties are

(Eq. 44)

$$\rho_0 = \frac{2116}{(53.3)(460)} = 0.0865 \text{ lb/ft}^3$$

$\mu_o = 1.10 \times 10\text{-}5$ lb/s-ft

$k_o = 0.0132$ Btu/h-ft-°F

Therefore $N_{(Re,o)} = \dfrac{1.69 \times 0.0865 \times 250 \times 2.0}{1.10 \times (10^{-5})} = 6.65 \times 10^6$

From Equation 11, transition occurs at

$$s = \left(\frac{1.5 \times 10^6}{6.65 \times 10^6}\right)\left(\frac{24.0}{\cos 21.8 \text{ deg}}\right) = 5.75 \text{ inches}$$

Therefore, s = 15.0 inches is in the turbulent region.

3. Compute local heat transfer coefficient. From Figure 13,

$$\frac{N_{Nu}}{(N_{(Re,o)})^{0.821}} = 0.0210 \quad \text{(Eq. 45)}$$

and therefore $h_o = \frac{0.0210(6.65)^{0.821} \times 10^{4.92} \times 0.0132}{2.0}$ = 52.1 Btu/h-ft^2

4. Compute power requirements. Using data obtained in steps 1 and 3,

$$\frac{M_\beta}{h_o} = \frac{11.8}{52.1} = 0.226 \quad \text{(Eq. 46)}$$

From Figure 21,

$$\text{Local } \frac{q/S}{h_o} = 67 - 11 = 56$$

Since 1 W/in^2 = 492 Btu/h-ft^2, the required local power intensity is

$$\frac{q}{S} = \frac{56 \times 52.1}{492} = 5.9 \text{ W/in}^2$$

10. WINDSHIELD ICE PROTECTION

10.1 Introduction

Anti-icing protection is usually provided for the forward-facing windshield panels on both military and commercial aircraft that are required to operate in all-weather conditions. The most widely used system is electrical anti-icing, whereby electric current is passed through a transparent conductive film that is part of the laminated windshield. The heat from the anti-icing film also prevents internal fogging for most configurations. Use of electrical heat also maintains the windshield interlayers (of a glass/vinyl laminated windshield) at near the optimum temperature for resistance to bird strikes (bird proofing).

Where adequate electric power is not available or when the windshield configuration does not allow use of electrical anti-icing at a feasible cost, the most common alternates are use of an external air blast system (that may also be used for rain removal) or use of a fluid anti-icing system using freeze-point depressant solutions (such as glycol or alcohol) to prevent freezing of impinging water. Hot air flowing through a double pane windshield has been used for anti-icing in the past, but is seldom used currently because of problems of installation, noise, collection of dirt between panes, and other undesirable effects.

The following paragraphs describe in detail the various methods of providing windshield ice protection, with typical examples. Methods of analysis, equations, and typical results are also shown.

10.2 Methods of Protection

10.2.1 Electrical Anti-Icing

Heating is accomplished by applying electric power to a conductive transparent film located on the inner surface of the outer ply. This ply is usually limited to 0.18 inch thickness if the surface is glass (or 0.06 inch if plastic), to avoid excessive internal temperatures. Power supply bus bars and the temperature control sensor are usually located as shown in Figure 29.

Power input must be adequate to maintain a running wet surface (35 °F) under the design icing condition. A power input of 3 to 4.5 W/in^2 is normally used, and will give satisfactory protection for most icing conditions. Some civilian regulatory guidance suggests that a nominal density of 4.5 W/in^2 (70 W/dm^2) is adequate. Designs should consider system tolerances (power delivery and heater resistance tolerances), particularly on lower voltage DC power systems. Higher heat inputs may have an adverse effect on windshield service life because of increased thermal stresses resulting when power is applied and removed. Thus the minimum heat input that will give icing protection should be used.

Power supply is normally from an AC generator; however, if only DC power is available, an inverter can be used to produce the required voltage when using a conductive film heater element. Alternately, DC powered windshields are available with very small filament heating elements embedded between layers. Filament heater designs can have some limited visual distortion effects. Acceptability may require evaluation. The temperature control is set at a value high enough to produce the design heat requirement without overheating the interlayer. Usually a setting of 110 to 120 °F will fulfill both the anti-icing and antifog temperature requirements for glass outer ply construction. The most common control turns full power on and off as necessary to maintain the set temperature within a 10 °F dead band. Controlling in this manner may result in cyclic thermal stresses that have adverse effects on windshield service life. Reducing thermal stresses is a major consideration in designing for service life. Windshields with an acrylic outer ply are more sensitive to heater temperature excursions as the acrylic is less conductive and has more thermal inertia than glass outer plies. Some designs have additional compensations, such as higher frequency power modulation, more precise thermal control (±1 °F), as well as dual set points (lower temperatures for defog operation) to minimize heater temperatures and extend service life.

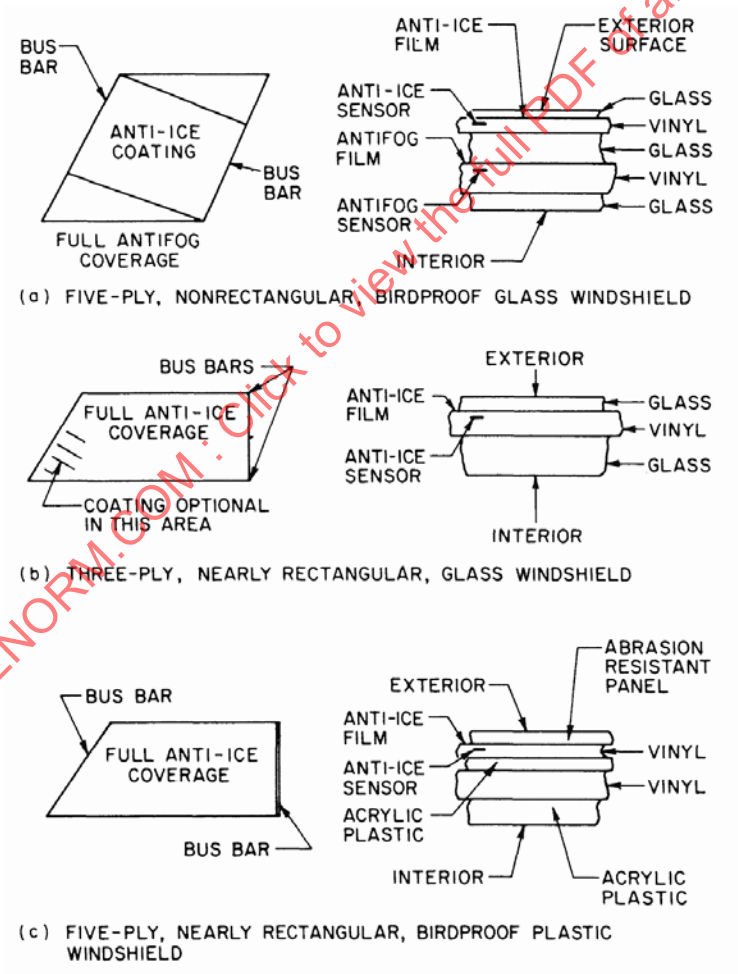

Figure 29 - Typical windshield panels heated electrically

An important factor in determining windshield requirements is how large of an area needs protection. ARP4101/2 (Reference 23) provides some recommendations for determining adequate pilot compartment view. The power requirements can impact power generation system design, particularly on general aviation aircraft.

Some current aircraft are using modulating controls that vary power as a function of temperature sensor demand, to reduce thermal stresses.

Successful design of a windshield having electrical heating requires careful integration of all factors involved. The most important are: providing good coating uniformity (use of nearly rectangular areas), limiting heat input to the minimum acceptable level, and, if possible, using a modulating control to eliminate cyclic thermal stresses. Methods of calculating the heat required and temperature control setting are shown in 10.3.1 together with a calculation method to determine temperature of the interlayer.

10.2.2 Hot Air Anti-Icing

10.2.2.1 Double Pane Anti-Icing System

Although seldom used, the double pane system (Figure 30) is a possible alternative to electrical anti-icing. A source of hot air is needed (such as a combustion heater, or compressor bleed diluted or cooled to an acceptable temperature), with a control valve and appropriate ducting. Surface heat requirements are the same as for an electrical system; however, the total heat input will be two or three times as large, depending on air gap width and resulting channel efficiency. Methods of analysis shown in 5.3 for airfoil anti-icing may be used to determine air flow requirements.

Special attention must be given to solution of the problems of noise, duct installation, leakage, accumulation of dirt, dust, and oil, and stress problems resulting from temperature gradients in the windshield panes.

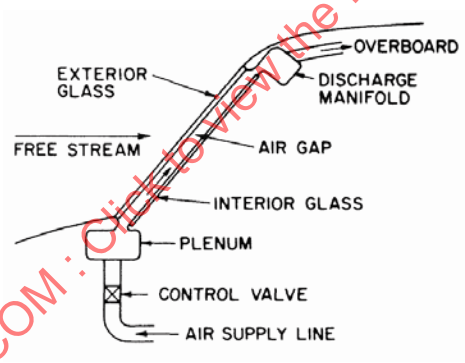

Figure 30 - Double pane hot air windshield anti-icing system

10.2.2.2 External Air Blast Anti-Icing

For many high performance aircraft, an external jet blast rain removal system employing compressor bleed air is used in place of windshield wipers (see Section 12). The bleed air is discharged at the base of the windshield by a wide, narrow depth nozzle that directs air parallel to the windshield surface (Figure 31). Design of such systems is empirical to a large degree; however, general recommendations may be found in AIR805 (Reference 19). Air flow rates required are usually between 2 and 7 lb/min-in (width) of cleared area, with values of 4.5 to 7 lb/min-in giving the most satisfactory results for rain removal.

In most cases, rain removal air flow requirements will exceed windshield anti-icing requirements. Typical surface temperatures are discussed in 10.3.2.2. Care must be exercised in designing such a system, to avoid blowing excessively hot air across the windshield. This can cause overheating of the interlayer or cracking of the outer glass ply, or thermal damage to acrylic windshields.

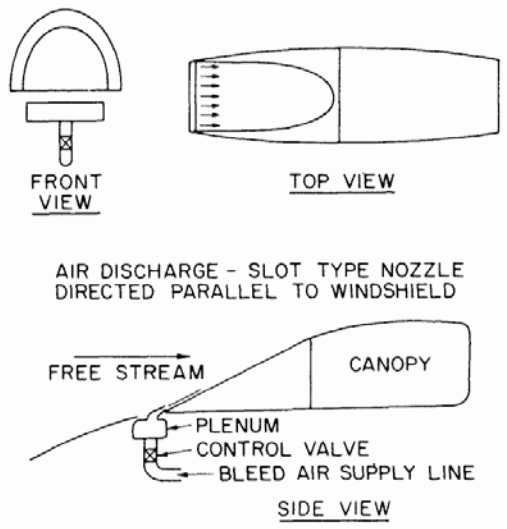

Figure 31 - External air blast windshield anti-icing and rain removal system

10.2.3 Fluid Anti-Icing

For many applications, electric power or hot air may not be available in sufficient amounts for anti-icing, and a fluid anti-icing system may be a suitable alternative. It is a simple system for retrofit applications, and the weight increase for non-icing flight missions is small because the fluid can be drained. The fluid system prevents ice by spreading sufficient fluid over the windshield so that the impinging water plus anti-icing fluid has a freezing point lower than the windshield surface temperature. Typical fluids are ethylene glycol, isopropyl alcohol, ethyl alcohol, and methyl alcohol. Various proprietary fluids are also available.

The fluid is most commonly distributed by a small "piccolo" tube with evenly spaced holes, or by one or more spray nozzles, or by a porous metal strip. Pressure to force the fluid through the distribution system may be supplied by a small pump or bleed air, if available.

Although designed for anti-icing protection (that is, the system is turned on when icing is encountered), the fluid system may also be used for deicing, to remove ice accumulations. In this case the fluid and ice form a slush that is swept away by aerodynamic forces. Fluid systems can alter the visibility through the windshield, and in some cases may require discontinuing use just prior to final approach to ensure adequate visibility.

10.3 Analysis of System Requirements

10.3.1 Electrical Anti-Icing

Current technology allows the use of computational fluid dynamic methods to predict local and total water catch efficiencies, considering the three dimensional effects of flow around a windshield. However, the following method provides the fundamental calculation methods.

Windshield water catch may be determined by Equation 4:

$$M_w = 0.38vA_F(LWC)E_m/A_w \quad \text{(Eq. 47)}$$

where M_w = lb/h-ft^2 of windshield surface area.

In this case A_F is the windshield projected area (along the line of flight). The impingement efficiency E_m is normally obtained from data for a semi-infinite rectangle. The graphs of Figures 32 and 33 allow rapid determination of E_m. Because impingement rate is of secondary importance in a running wet anti-icing system, further refinement of water catch is usually unnecessary.

The heat transfer coefficient at the center of the windshield heated area must also be determined. Experience has shown that, for windshields, the turbulent flow equation for a flat plate may be used. Equation 9 may be used to obtain the heat transfer coefficient at the center of the windshield; or the graph of Figure 11 may be used if the value for h_o from Equation 9 is multiplied by 0.8. The distance L_x is the distance from the base of the windshield to the center for nearly vertical windshields; or from the nose of the aircraft for inclined windshields (that is, where the angle between fuselage and windshield is not so severe as to generate a new boundary layer).

The heat required for a 35 °F surface temperature may be calculated using Equation 24. Typical values are shown in Figure 34. Anti-icing requirements for transparent areas are covered in Reference 16 for military aircraft and in Reference 33 for commercial aircraft. The requirements are a function of normal cruise speed, as shown in Table 2. (The corresponding watt intensities are included for reference only and do not imply that the system must be electrical. A hot air external jet blast is often used as a combination anti-icing and rain removal system.)

Table 2 - Heat requirements at various cruise speeds

	Heat Requirement	
Normal Cruise Speed, Knots	Btu/hr-ft^2	W/in^2
100	1200	2.44
150	1700	3.45
200	1900	3.86
250	2000	4.06
300	2100	4.26
Over 300	2100	4.26

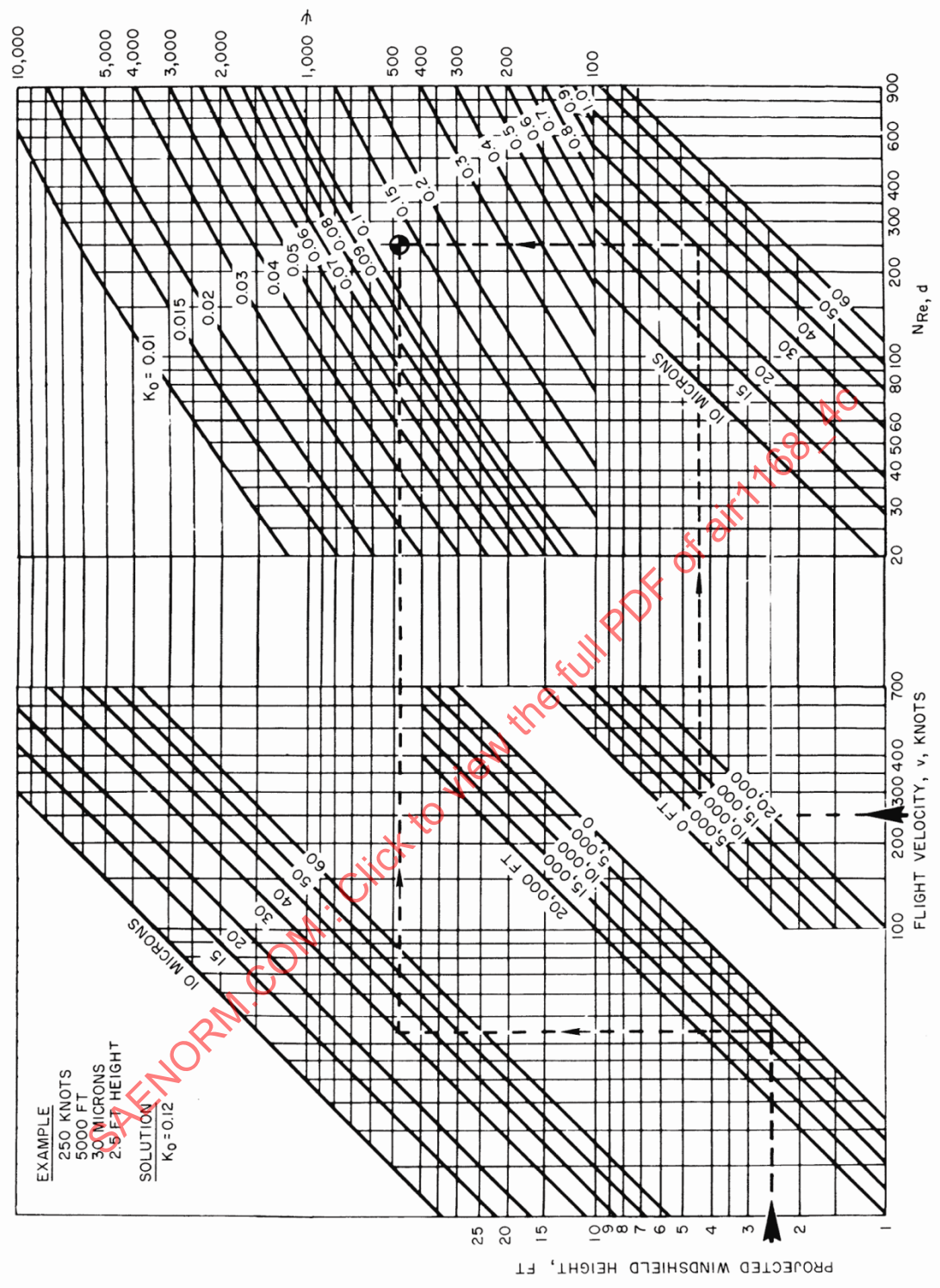

Figure 32 - Graphical solution of K_o for 15 °F ambient air temperature (References 6 and 7)

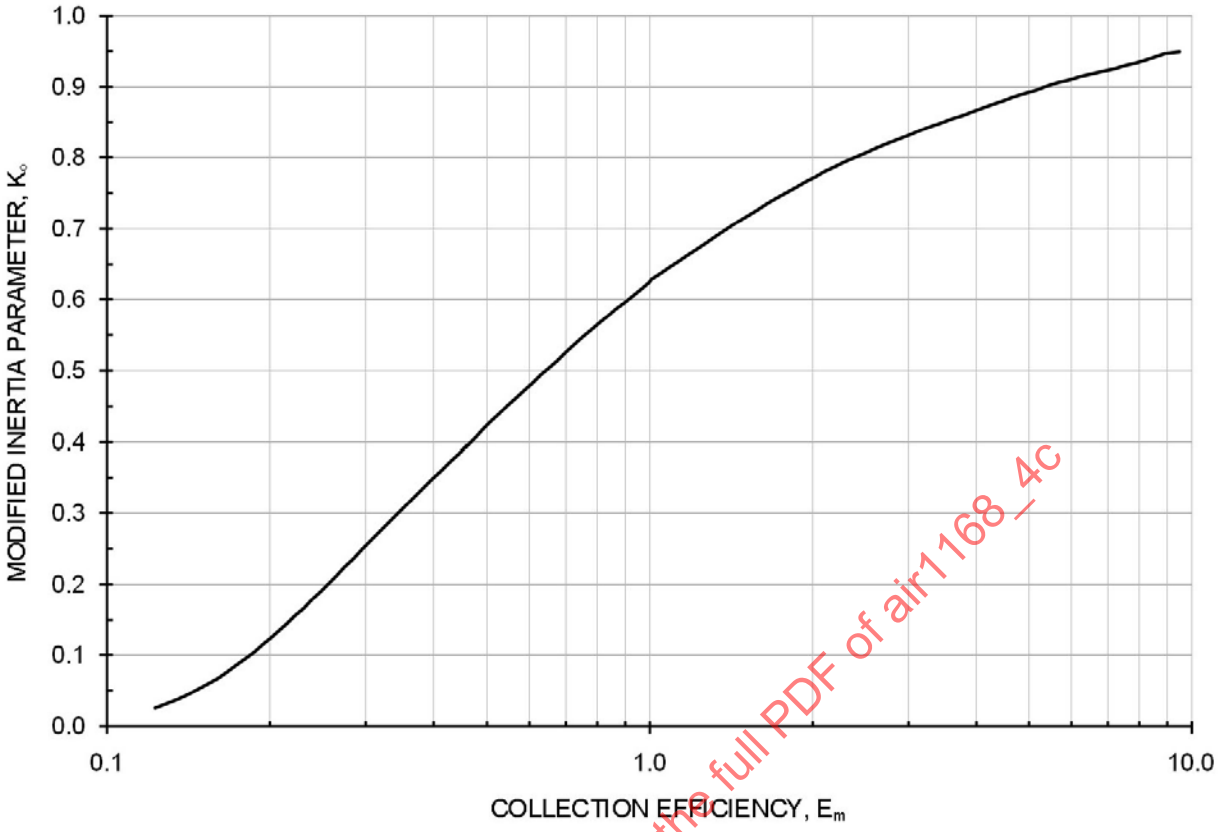

Figure 33 - Collection efficiency of windshields (based on semi-infinite rectangle)

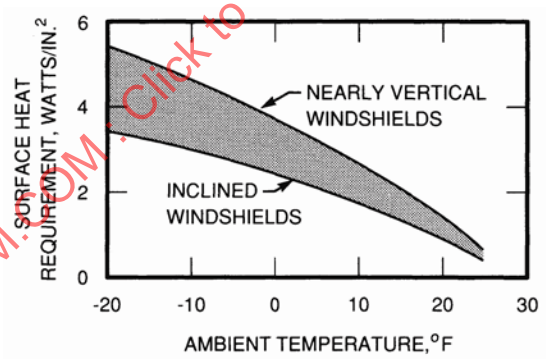

Figure 34 - Variation of windshield surface heat requirement with ambient temperature (calculated for 7000 feet cruise at 205 mph true air speed)

An additional correction is needed for inward heat flow to the cabin. This may be calculated after the anti-icing film temperature has been determined. In most windshields and for normal cabin temperatures, the inward heat loss is about 5% of the outward heat flow.

The characteristics of the anti-icing film are normally arrived at through consideration of practical conductive film manufacturing tolerances, the maximum hot spot temperature that must be set to avoid damage to the vinyl or glass, and the tolerances in control point temperature produced by the windshield temperature controller. These film characteristics are defined as the following power constants:

$$K_a = \frac{\text{Average power}}{\text{Power at control point}} = \frac{t_{fa} - t_s}{t_c - t_s} \quad \text{(Eq. 48)}$$

(Recommended K_a = 0.80 or greater.)

$$K_h = \frac{\text{Power at hot spot}}{\text{Power at control point}} = \frac{t_h - t_s}{t_c - t_s} \quad \text{(Eq. 49)}$$

(Recommended K_h = 1.3 or less.)

$$K_m = \frac{\text{Average power}}{\text{Power at hot spot}} = \frac{K_a}{K_h} \quad \text{(Eq. 50)}$$

(Recommended K_m = 0.7 or greater.)

For ideal (uniform) heating, the constants would be unity.

With known power (average) requirement and power constants, the film temperature at the control point and at the hot spot may be calculated. The average film temperature is

$$t_{fa} = t_s + \frac{q_a \Delta x_o}{k_g} \quad \text{(Eq. 51)}$$

for glass, where k_g is replaced by k_p if plastic is considered.

Similarly, the temperature of the film at the control point and hot spot may be found if K_a and K_h are known. Temperature at the hot spot is usually limited to 160 °F, to avoid damage to the vinyl.

For a windshield on a subsonic jet transport the recommended power constants will provide average outside windshield surface temperatures above 35 °F in the most probable icing conditions up to an altitude of 22000 feet with a control point setting of 105 to 110 °F and a conductive coating of 2100 Btu/h-ft^2.

The control sensor is usually mounted in the adjacent interlayer, 0.04 inch or less from the film. Sensor temperature will be within 2 °F of the film temperature at this point.

Interlayer temperatures may be calculated, if needed, for windshield bird-impact considerations, from the film temperature, average total heat flow, and conventional two-dimensional heat transfer equations. A heat transfer coefficient of h = 2 Btu/h-ft^2-°F is usually appropriate for the inside face of the windshield.

Windshield power control may use either of two principles. Most common is the "on-off" cycling control, which turns full power on and off as needed to maintain a desired control temperature (typically ±5 °F around the control point). A more complex control may be used to modulate power according to sensor demand, and may include a "warmup" control to apply power gradually to a cold windshield. This control minimizes the cyclic thermal stresses that cause glass breakage.

10.3.2 Hot Air Anti-Icing

10.3.2.1 Double Pane Hot Air Anti-Icing

Heat requirements for a double pane hot air anti-icing system are obtained by the method described for electrical anti-icing. With a selected source of hot air, the problem is simply that of varying the air flow rate and air gap until a satisfactory compromise is made between heat release and pressure drop. A heat exchanger efficiency of 50% is a realistic goal. Internal heat transfer coefficients may be calculated from equations presented in 5.3.

Air flow should be from the base of the windshield upward, so that maximum heat release is achieved at this point. Assuming that the gap must be of uniform thickness for optical reasons, the heat release rate will decrease with distance along the windshield.

10.3.2.2 External Air Blast Method

The external air blast system will normally be designed for rain removal by either laboratory development or use of empirical design data such as References 19 and 20. The problem remaining usually is the analytical evaluation of the rain clearing system under icing conditions. As a first approximation, the data of Figure 35 may be used to estimate surface temperatures. For other configurations, consult Reference 20. In most cases, air flow and temperature requirements for anti-icing are less severe than for rain clearing.

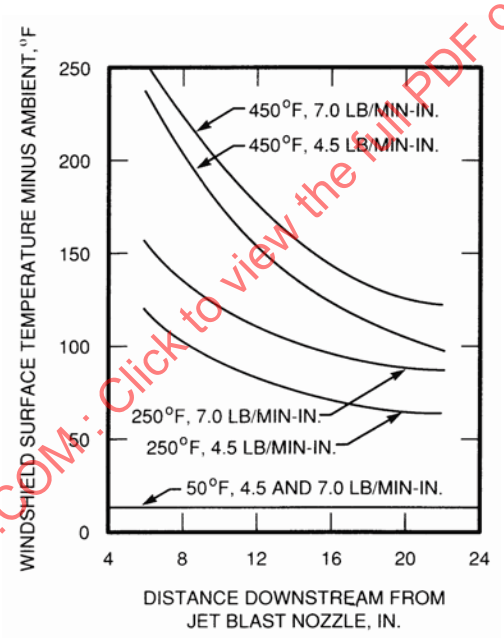

Figure 35 - Windshield surface temperature in icing for external air blast anti-icing system. Flight velocity, 225 knots; liquid content, 1.0 g/m³; nozzle velocity, Mach 1; drop size 20 µm, continuous slot nozzle

10.3.3 Fluid Anti-Icing

The water catch on the windshield per unit area of windshield surface must be determined, as discussed in 10.3.1. The reference (datum) temperature may be determined from the approximate graph of Figure 36. From Figure 37 (obtained from Reference 8), the percent of freezing point depressant by weight (G_f) may be found. This is the amount of fluid required to mix with impinging water to result in the selected freezing temperature. The flow rate required is

$$W_f = \frac{G_f M_w}{G_i - G_f} \quad \text{(Eq. 52)}$$

Thus, for a datum temperature of 0 °F and 0.57 lb/h-ft^2 impingement (for 50/50 ethylene glycol/water, G_i = 50%), and from Figure 37, at 0 °F, ethylene glycol, G_f = 35%. Then

$$W_f = \frac{(35)(0.57)}{50-35} = 1.33 \text{ lb/h} - \text{ft}^2$$

For two 18 inch square windshield sections, the flow for 4.5 ft^2 is 6.0 lb/h. Actual flow may have to be 1.2 to 1.5 times greater, depending on distribution efficiency.

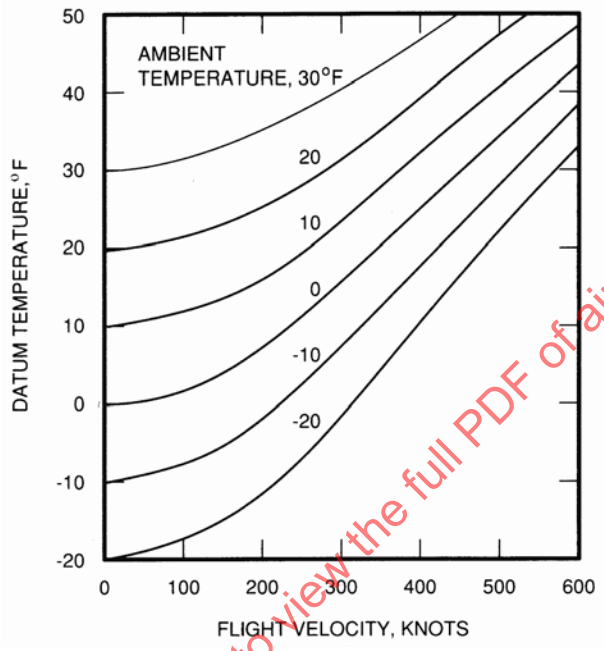

Figure 36 - Datum temperature versus flight velocity (values shown at 10000 feet and are approximately correct for 0 to 20000 feet; see Reference 8)

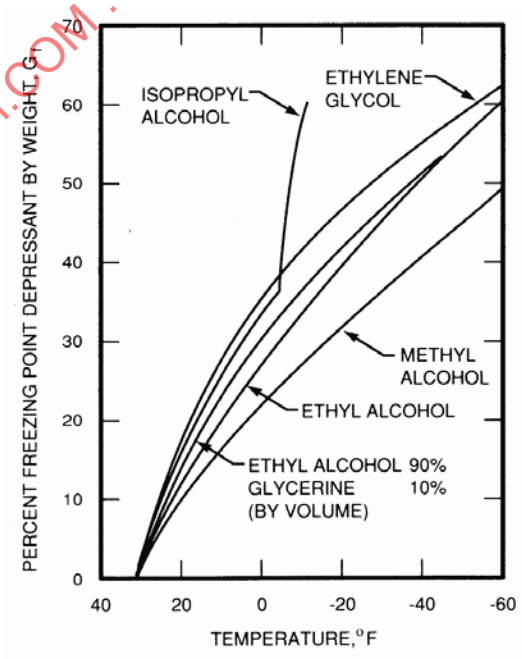

Figure 37 - Freezing points for aqueous solutions of several fluids

Tank capacity must be adequate for expected duration in icing plus a reserve. Continuous icing conditions seldom exist for a distance exceeding 200 miles. (Note that the maximum cloud extent cited in references 12 and 41 is 310 nautical miles.) Hold in icing must also be considered. Current FAA policy is to consider a 45-minute hold (a 30-minute hold for helicopters) in a standard extent Continuous Maximum cloud. There are also recommendations on tank capacity, see Reference 36 or later revision for current regulatory guidance. For military aircraft tank capacity should be consistent with the mission of the aircraft.

11. WINDSHIELD AND CANOPY FOG AND FROST PROTECTION

11.1 Introduction

The inner surfaces of most cockpit transparencies are susceptible to condensation in the form of fog or frost during normal aircraft operation, particularly when descending from a high altitude flight, unless fog and frost protection systems are provided.

Two distinct approaches can be taken to provide the flight crew with clear vision areas. One is to keep the inner surface of the transparency continuously above the maximum anticipated cabin dew point; this is the "antifog" system. The other approach is to energize the system only after fog or frost has formed; this is the "defog" system. As a general rule, antifog systems are preferred because they keep windows clear at all times.

The two most common and practical methods are the use of electrical heating and the "free jet" hot air blast system. In many cases use of the electrical anti-icing system for a windshield will keep the inner surface warm enough to provide fog and frost protection. Electrically heated panels offer the best protection with the least effect on cabin temperature, and generally provide quite uniform temperatures. Cost of installation and in-service replacement of the heated panels and controls are the major objections to use of electrical heating.

The "free jet" system is commonly used where a source of compressor bleed air is available. Bleed air is mixed with cabin air by an ejector to yield a safe air temperature (usually below 200 °F). The mixed air is discharged through a slot type of nozzle over the inner surface of the windshield, and will maintain an area clear for about 1 to 3 feet (depending on flow rate and design conditions). Although simple to install, the free jet hot air system has the disadvantage of noise, increased cabin temperature, and increased cabin free air velocity.

Other possibilities, depending on the specific application, are double pane hot air heating, use of dehydrated air, infrared heating, and "antifog" chemical coatings.

The following paragraphs describe the two main methods of fog protection (electrical and free jet hot air), methods of analysis, and typical electric power and air flow requirements. A discussion of the other methods is also included, with comments on specific applications.

11.2 Methods of Fog Protection

11.2.1 Electrical Heating

If electrical heating has been selected for windshield bird proofing or ice protection, the antifog problem is reduced to that of an analysis of inside surface temperature and cabin dew point for low ambient temperature conditions. The object is to determine whether the control temperature setting for anti-icing will maintain the inside surface temperature above the cabin dew point. Data on electrical anti-icing has been presented previously in 10.2.1 and 10.3.1.

Even though a steady-state analysis will often show that the anti-ice coating will provide inside surface temperatures above the cabin dew point, the addition of an antifog coating may be desirable to reduce the time needed to reach bird proofing temperatures prior to take-off.

For a canopy, windshield, or camera window that is not already electrically heated for anti-icing or bird proofing, electrical antifog protection may be used. A typical laminated plastic panel with antifog electrical coating is shown in Figure 38. Bus bars are located in noncritical vision areas. Because the power input is low (1/2 to 1 W/in^2), nonrectangular areas may be protected with little danger of overheat. Temperature uniformity is always best for rectangular areas, however.

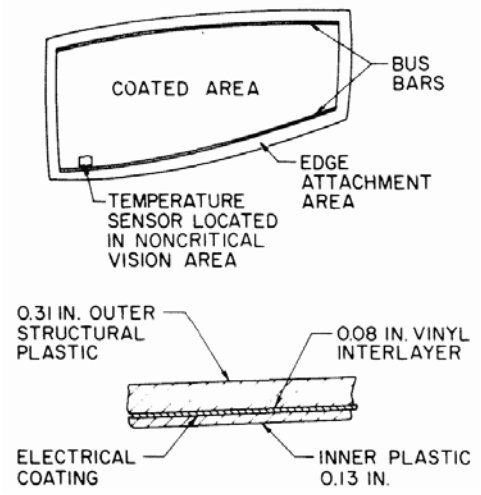

Figure 38 - Antifog coating and bus bar arrangement for electrical antifog on plastic canopy (or windshield) panel

Power input and sensor temperature setting must be greater than that required for the most severe combination of ambient temperature, humidity, flight speed, and cabin temperature. For high performance aircraft, 1 W/in^2 and 90 °F, respectively, are typical values, with lesser requirements for less severe flight profiles, or with thicker structural plies outboard of the conductive coating (which reduce the external heat losses). Methods of calculating requirements are given in 11.3.2 and 11.3.3.

For windshields or canopies having the conductive coating located near the inner surface, a simple temperature control system can be used, consisting of a bimetallic surface-mounted snap switch wired in series with the conductive coating. This eliminates the need for more costly and heavy relays and controllers. Where the plastic coating is located more than about 0.15 inch from the inner surface, or about 0.4 inch for glass, or where more accurate temperature regulation is desired, internal sensing elements connected to appropriate controllers and relays are needed.

11.2.2 Free Jet Air Blast

The free jet air blast system is commonly used in jet aircraft because of the ease of installation, lower cost of the non-electrical windshield and canopy panels, and availability of engine compressor bleed air. The normal installation uses bleed air, reduced to about 8 to 10 psi above cabin pressure and driving an ejector that draws in sufficient cabin air to produce a mixed temperature (200 °F), below the softening point of plastic.

Mixed air is discharged through a plenum nozzle assembly as shown in Figure 39. A typical flow rate for a canopy panel on a high-speed aircraft would be 0.4 to 0.5 lb/min-in of panel width. The corrugated insert shown in the nozzle may be used to adjust flow for equal distribution over the length of the nozzle.

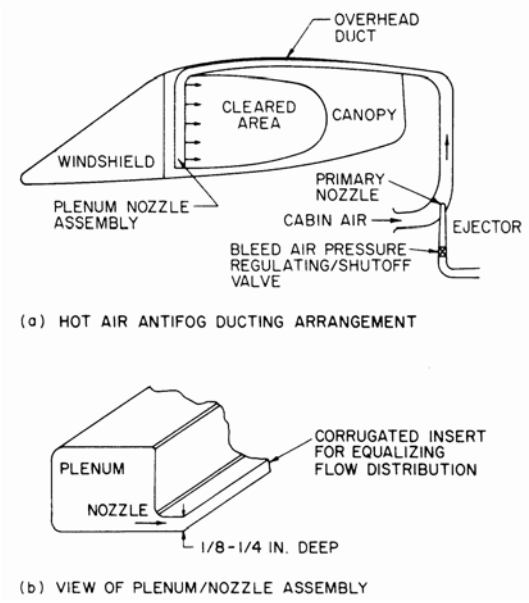

Figure 39 - Free jet air blast antifog or defog system using mixed compressor bleed and cabin air

It is important that the nozzle be designed to contact the window or the frame so as to prevent the air blast from ejecting ambient cabin air between the nozzle and the window. This will increase the effectiveness of the air blast.

Calculation methods for steady-state and transient operation are discussed in subsequent paragraphs (11.3.3 and 11.3.4).

11.2.3 Double Pane Hot Air

Antifog protection would be obtained if a double pane hot air anti-icing system (as outlined in 10.2.2.1 and 10.3.2.1) is installed. The installation difficulties and weight of such a system used for antifog only will limit its usefulness. Calculation of heat requirements is outlined in 11.3.3.

11.2.4 Dehydration of Defogging Air

Another approach that has merit for certain applications is dehydration of the defogging air. The object is to form a "buffer" layer of dry air interposed between the inner surface of the windshield and the potential moisture source (cabin). A slot type of nozzle, or closely spaced holes, may be used to inject air parallel to the inside surface, as with the "free jet" hot air antifog system (Figure 39).

Possible dehydrated air sources are: stored dry nitrogen (bottle), conditioned air from the main aircraft system (which would be dry at high altitudes), and air from any source passed through silica gel or an activated alumina bed, as discussed in Reference 21.

Use of dehydration systems is usually limited to short duration applications or "one of a kind" installations. Determination of flow rate required for protection is somewhat empirical; however, the air velocity decay versus distance can be used as a guide to the proper selection of flow rate, using the equation of 11.3.3.2 for velocity decay.

11.2.5 Infrared Heating

Use of an infrared heat source to apply heat to a transparent area is often suggested, but no practical applications are known to have been made. Heat requirements may be determined by methods of 11.3.3. Efficiency may be between 50 and 80%, according to Reference 22.